AD-A089 947 MASSACHUSETTS UNIV AMHERST DEPT OF POLYMER SCIENCE --ETC F/G 11/9
STUDIES OF POLYURETHANES AND EPOXY CURING REACTIONS.(U)
AUG 80 W J MACKNIGHT DAAG46-79-C-0004

UNCLASSIFIED AMMRC-TR-80-43 NL

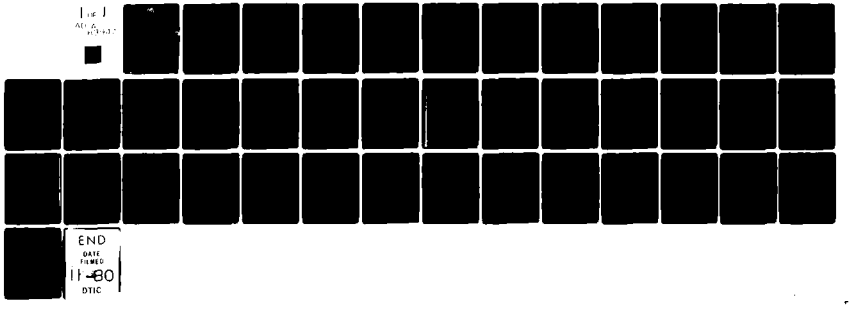

END
DATE FILMED
11-80
DTIC

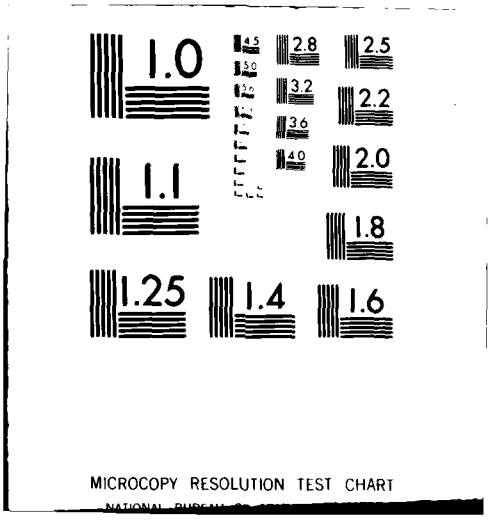
1.0
1.1
1.25
1.4
1.6
1.8
2.0
2.2
2.5
2.8
3.2
3.6
4.0
4.5
5.0
MICROCOPY RESOLUTION TEST CHART

LEVEL II

12

Report AMMRC TR 80-43

STUDIES OF POLYURETHANES AND EPOXY CURING REACTIONS

William J. MacKnight

Polymer Science and Engineering Department
University of Massachusetts
Amherst, MA 01003

August 1980

Final Report: 15 October 1978 - 15 October 1979

Approved for public release; distribution unlimited.

Prepared for:

Army Materials and Mechanics Research Center
Watertown, MA 02172

ONRRR, Harvard University
Gordon McKay Laboratory, Room 113
Cambridge, MA 02138

Unclassified

SECURITY CLASSIFICATION OF THIS PAGE (When Data Entered)

REPORT DOCUMENTATION PAGE	READ INSTRUCTIONS BEFORE COMPLETING FORM
1. REPORT NUMBER: AMMRC TR-80-43	2. GOVT ACCESSION NO. / 3. RECIPIENT'S CATALOG NUMBER
4. TITLE (and Subtitle): Studies of Polyurethanes and Epoxy Curing Reactions,	5. TYPE OF REPORT & PERIOD COVERED: Final Report, Oct 78 – 15 Oct 79
	6. PERFORMING ORG. REPORT NUMBER
7. AUTHOR(s): William J. MacKnight	8. CONTRACT OR GRANT NUMBER(s): DAAG 46-79-C-004
9. PERFORMING ORGANIZATION NAME AND ADDRESS: Polymer Science & Engineering, ~~Department~~ University of Massachusetts Amherst, MA 01003	10. PROGRAM ELEMENT, PROJECT, TASK AREA & WORK UNIT NUMBERS: D/A Proj. 1L161102AH42 AMCMS Code: 611102.11.H42
11. CONTROLLING OFFICE NAME AND ADDRESS: Army Materials & Mechanics Research Center Watertown, MA 02172	12. REPORT DATE: Aug 1980 / 13. NUMBER OF PAGES: 13
14. MONITORING AGENCY NAME & ADDRESS (if different from Controlling Office): 42	15. SECURITY CLASS. (of this report): Unclassified / 15a. DECLASSIFICATION/DOWNGRADING SCHEDULE
16. DISTRIBUTION STATEMENT (of this Report): Approved for public release; distribution unlimited	
17. DISTRIBUTION STATEMENT (of the abstract entered in Block 20, if different from Report)	
18. SUPPLEMENTARY NOTES	
19. KEY WORDS (Continue on reverse side if necessary and identify by block number): Epoxy resins; Curing; Rates; Polyurethane Resins; Mechanical Properties; Polybutadiene; Transition Temperature	

20. ABSTRACT (Continue on reverse side if necessary and identify by block number)

The research performed by the Polymer Science and Engineering Department at the University of Massachusetts (Amherst) during the period 10/15/78 to 10/15/79 is summarized in this report. The work was supported by U.S. Army Contract DAAG-46-79-C-0004 from the Army Materials and Mechanics Research Center, Watertown, MA, with Dr. Nathan Schneider serving as the contracting officer's representative.

DD FORM 1 JAN 73 1473 EDITION OF 1 NOV 65 IS OBSOLETE

Unclassified 406 718

20. Abstract (continued)

The research objectives under this contract were:

(1) to synthesize several polybutadiene-containing polyurethanes and their hydrogenated derivatives and characterize them using dynamic mechanical and infrared analyses;

(2) to study in detail the cure mechanism for a particular epoxy resin using dynamic mechanical relaxation techniques.

Infrared and dynamic mechanical studies support the hypothesis that the polybutadiene-containing soft phase of these polyurethanes is relatively free of intermixed hard segments. The hydrogenated derivatives of these polymers appear to contain some crystallinity within the soft segment.

The kinetics of the curing reaction of an epoxy resin composed of diaminodiphenyl sulfone and tetraglycidyl 4,4' diaminodiphenyl methane epoxide was studied using dynamic spring analysis. The curing reaction was found to be first order; activation energies were determined.

TABLE OF CONTENTS

IV. FIGURES AND TABLES

Figure Captions

FIGURE 1: Infrared Spectrum of HTPBD Prepolymer

FIGURE 2a: Infrared Spectrum of Hydrogenated HTPBD Prepolymer

FIGURE 2b: Infrared Spectrum of Hydrogenated HTPBD Prepolymer Showing the 729 cm^{-1} Band

FIGURE 3: Infrared Spectrum of HTPBD-Containing Polyurethane Sample

FIGURE 4: Infrared Spectrum of Hydrogenated HTPBD-Containing Polyurethane Sample

FIGURE 5: Infrared Absorption Peak at Room Temperature of the NH and C=O Region

FIGURE 6: Temperature Dependence of the Storage and Loss Modulus for HTPBD-Containing Polyurethanes (6a) and their Hydrogenated Derivatives (6b) at 11 Hz

FIGURE 7: Temperature Dependence of the Loss Tangent for HTPBD-Containing Polyurethanes (7a) and their Hydrogenated Derivatives (7b) at 11 Hz.

FIGURE 8: Stress-Strain Response of HTPBD-Containing Polyurethanes (———) and Their Hydrogenated Derivatives (-----)

FIGURE 9: Cyclic Stress-Strain Curves for (a) R-51 (HTPBD-Containing Polyurethane); and (b) HY-51 (Hydrogenated Derivative) Extended 20, 40, 60, and 80% ε_b

FIGURE 10: Tan δ versus ln(t) (Seconds) at Four Frequencies, 147°C

FIGURE 11: Tan δ versus ln(t) (Seconds) at Four Temperatures, 3.5 Hz

FIGURE 12: Tan δ versus Temperature (11 Hz) for Five Different Molecular Weights of Polystyrene

FIGURE 13: Storage and Loss Moduli versus ln(t) (Seconds) at Two Frequencies, 147°C

FIGURE 14: $\ln(t_{max})$ versus 1/T (Arrhenius Plots)

FIGURE 15: Logarithmic Viscosity versus Time (Seconds) at Four Temperatures

I. STRUCTURAL AND MECHANICAL PROPERTIES OF POLYBUTADIENE-CONTAINING POLYURETHANES

A. Introduction

Segmented polyurethanes which incorporate polybutadiene (PBD) as the soft segment, rather than polyether, are becoming increasingly important in a variety of specialty applications which require low moisture permeability. In particular, there have been a number of studies which have emphasized the potential of these polyurethanes as electrical potting compounds or adhesives (1-3). The hydroxyl terminated polybutadiene (HTPBD) used in these studies to synthesize polyurethanes contains 60% trans, 20% cis and 20% vinyl double bonds (4-6). The number average molecular weight is in the range of 2,800 and the average hydroxyl functionality between 2.1 and 2.3. Although the physical properties which result on curing this HTPBD with appropriate reagents to form polyurethanes are adequate for many applications, the tensile strength, tear strength and abrasion resistance are somewhat inferior to those of typical polyester and polyether urethane elastomers.

This report represents part of a continuing study relating the composition and phase segregation behavior to the properties of segmented polyurethanes (7). The incorporation of HTPBD as the soft segment rather than polyethers or polyesters has the advantages for property studies of restricting hydrogen bonding to the hard segment only and of promoting phase segregation. Dynamic mechanical properties and stress-strain behavior of such polymers are examined. Also investigated is the effect of hydrogenation of the HTPBD on the properties of these polybutadiene polyurethanes.

B. Experimental

1. Materials and Polymerization Conditions

The synthesis was carried out by a two step method involving endcapping the hydroxyl-terminated polybutadiene (PBD)(Arco, R45M) with a 5% molar excess of toluene-2,4-diisocyanate (TDI)(Aldrich) followed by reaction with the chain extender, 1,4 butanediol (BDO) (Aldrich).

A 100 ml reaction vessel equipped with a mechanical stirrer and vacuum outlet was charged with liquid prepolymer, evacuated and immersed in an oil bath at 120°C. After one hour, a weighed amount of TDI was added. The mixture was then stirred for one hour under constant nitrogen flow, after which the temperature was lowered to 80°C. Following the addition of the chain extender, BDO, the reation mixture was degassed, poured between teflon sheets and cured in air at 120°C for 17 hours.

2. Hydrogenation of Prepolymer

HTPBD (100 g) was dissolved in 500 ml of toluene in a 2 liter reactor sleeve. Approximately 0.5 g of Pd on activated charcoal catalyst was added and the sleeve was placed in the pressure reactor bomb assembly to which a hydrogen cylinder was connected. The vessel was purged with H_2 for 15 minutes and then pressurized with H_2. The reaction was allowed to proceed until a pressure drop was attained which corresponded to the desired level

of hydrogenation. The mixture was then filtered through a Buchner funnel and the catalyst residues were removed. The solvent was evaporated with a rotary evaporator, isolating the hydrogenated polybutadiene prepolymer (HYPBD).

The extent of hydrogenation was determined by microanalysis for carbon and hydrogen and by proton nuclear magnetic resonance (NMR)

3. Infrared Analysis

Infrared spectra (400 - 4000 cm^{-1}) were obtained with a Nicolet 7199 Fourier Transform Infrared spectrometer. One hundred scans at 2 cm^{-1} resolution were signal averaged and stored on a disk for further analysis. Spectra of the prepolymer and its hydrogenated form were obtained from films cast from chloroform solution on KBr disks. Usually this technique yields sufficiently thin films for quantitative analysis. The criteria for the analysis is that Beer's law be obeyed; hence low absorptions are needed (8). Identical infrared spectra were also obtained for films cast from the melt at 25°C. However, this technique usually yields thicker films, and hence higher absorbance values. Since the polyurethanes prepared were insoluble, the reaction mixtures were degassed and pressed between two KBr disks or aluminum plates. Samples thin enough for spectroscopic analysis can be obtained by this procedure.

4. Dynamic Mechanical Measurements

All measurements were carried out using a Vibron Dynamic Viscoelastomer (Toyo Measuring Instrument Co.) Model DDV II at a fixed frequency of 11 Hz. The temperature range was from -130°C to 120°C and the samples were heated at a nominal rate of 1.5 deg/min under a dry nitrogen atmosphere.

5. Tensile Testing

Stress-strain data were obtained on an Instron Model TM-SM table model universal testing instrument at an extension rate of 40 mm/min. Specimens were die-cut from a sheet of the polyurethane film .015 in. thick. A specimen gage length was about 1.5 in. long and .12 in. in width. In cyclic stress-strain experiments, a single sample was submitted to increasing amounts of prestrain. The sample was extended by increments up to 20%, allowed to relax at zero load for 5 minutes, extended to 40%, etc. This test provides data at 0, 20, 40, 60 and 80% of the extension at break (ϵ_b).

C. Results and Discussion

Two series of polyurethanes were prepared; one based on the HTPBD and the second on the HYPBD prepolymer. Each consisted of three samples with a stepwise increment of TDI and BD relative to the prepolymer and at NCO/OH ratio of approximately 1.05, assuming a functionality of 2.1 hydroxyls per molecule for the prepolymer (see Table I).

The percent of hydrogenation of the prepolymer as determined by microanalysis and NMR was 65%.

1. Infrared Analysis

The infrared spectra confirmed the composition expected for the prepolymer. The strong 970 cm^{-1} and 910 cm^{-1} bands are generally associated with the C-H out of plane motion in the trans and 1,2 vinyl units, respectively (9). In addition, the 995 cm^{-1} band was used to analyze the cis content (10). These normal motions are very localized and, therefore, suitable for quantitative analysis (9).

After hydrogenation, significant changes in the ratios of these bands are observed. For example, as shown in Figures 1 and 2a, the integrated intensity of the 910 cm^{-1} band, assignable to 1,2 vinyl group, decreased substantially compared to trans segments; the ratio of the integrated intensities of 910 cm^{-1}/970 cm^{-1} decreasing from about 0.35 to 0.11 in the hydrogenated form. The preferential hydrogenation of the vinyl groups is in accord with the fact that this moiety occurs in a pendant position on the polymer and should be more accessible to hydrogen. This is consistent with the findings of Mango et al. in which the rate of hydrogenation of the vinyl double bond was found to be greater than that of the internal olefin (11). Although to a lesser extent than the vinyl group, the cis units were also preferentially hydrogenated over the trans. In addition, the 1377 cm^{-1} band associated with methyl rocking motion was detected after hydrogenation (12).

The sequence length of the methylene units in the hydrogenated samples was also of interest. A medium intense band was found at 720 cm^{-1}, which is commonly associated with amorphous polyethylene (13,14). This observation suggests that hydrogenation is quite extensive, consistent with the NMR studies, which showed a 65% saturation. In addition, a very weak band was observed at 729 cm^{-1} as shown in Figure 2b. This band is the CH_2 rocking vibration component arising from the crystal field splitting associated with methylene sequences in an orthorhombic unit cell (14) The lack of extensive crystallinity is probably due to the random placement of the 1,2 vinyl groups and residual unsaturated segments within the polymer chain.

As shown in Figures 3 and 4, the spectra associated with the unsaturated and hydrogenated PBD polyurethanes are much more complicated. In the prepolymer, preferential hydrogenation of the cis and 1,2 vinyl groups was also observed. This behavior is identical for the three samples of varying hard segment concentration. However, the bands in the 720 - 730 cm^{-1} region are barely observable above the background for any quantitative analysis, as shown in Figure 4.

Two other regions of interest in the IR spectra of these polyurethanes are the N-H carbonyl absorption regions. The major N-H absorption appears at 3310 cm^{-1}, typical for hydrogen bonded N-H groups. A small shoulder on the high frequency side of this peak at around 3440 cm^{-1} arises from non-bonded N-H groups. Similar observations are found in the carbonyl region; absorption bands at 1733 and 1710 cm^{-1} being assigned to the free and bonded carbonyl groups respectively (see Figure 5).

Studies of a series of MDI (p,p'-diphenyl methane diisocynate) polyurethanes containing polyether and polyester soft segments by Seymour and coworkers (16) have shown that virtually all N-H groups were hydrogen bonded but that only 60% of the urethane carbonyl groups were similarly associated. They suggest that the N-H groups also hydrogen bond to the soft segment at the interface of the phase separated structure or in the soft segment itself due to incomplete phase separation. In these butadiene-containing polyurethanes however, hydrogen bonding occurs only to urethane segments since the carbonyl in the urethane linkage and the urethane alkoxyl oxygen are the only available proton acceptors. This simplifies matters considerably when one attempts to quantitatively determine hard and soft segment interactions. For the N-H stretching vibration the fraction of hydrogen bonded and free N-H groups was resolved using a nonlinear least squares analysis for the fitting of Lorentzian curve shapes with a Gaussian approximation of the absorption bands. After taking into account the extinction coefficiant difference (17), 90% of the N-H groups in the HY-51 polyurethane were found to be hydrogen bonded. This value increased slightly with hard segment content and was essentially the same in both the unsaturated and hydrogenated polyurethanes. Bonded N-H contents of 75 to 95% have been found for other polyurethanes at room temperature (16,18,19,20). The role of hydrogen bonding in determining the mechanical properties for these polyurethanes is currently being studied.

2. Dynamic Mechanical Measurements

Results for the dynamic mechanical and tensile properties of the series of PBD and HYPBD polyurethanes are collected in Table 1.

Figure 6 represents the temperature dependence of the tensile storage and loss moduli (E' and E") for the various PBD and HYPBD-containing polyurethanes. Both series display a single major relaxation, labeled α, and characterized by a decrease in modulus from about 1000 to 10 MPa over a narrow temperature range. The α relaxation occurs at -74°C for the unsaturated polymers and at -69°C for the hydrogenated ones, all determined at 11 Hz from the position of the E" loss maximum. This α relaxation is associated with the glass transition temperature (Tg) of the soft (butadiene) segment. Its temperature is independent of hard segment content, indicating that these polyurethanes are well phase separated. This conclusion is further substantiated by the fact that the soft segment Tg of the unsaturated polymer is only 7°C higher than that obtained for the pure HTPBD. The slight elevation in Tg above that of free polybutadiene can be accounted for by an anchoring effect imposed by the hard segment on the soft segment phase and/or by small amounts of intermixing between the two phases.

Futher examination of Figure 6 shows that as hard segment content increases, the storage modulus at temperatures above the α relaxation temperature also increases. A corresponding decrease in intensity of the tan δ peak accompanies such changes in hard segment content. These effects are much less marked in the case of the hydrogenated polymer than in the unsaturated polymers. The temperature at which the limit of measurement was reached, corresponding to a modulus value of roughly 10 MPa, showed a corresponding increase with hard segment content for both series. These observations are

consistent with findings for other phase segregated systems (21). The latter effect can be directly attributed to an increase in hard segment density and, possibly, improved organization which occurs with increasing hard segment content.

A more direct comparison between the hydrogenated and nonhydrogenated polymers can be made by inspection of the temperature dependence of the loss tangent shown in Figure 7 for the various samples. It is at once apparent that all the hydrogenated polymers show a decrease in intensity and a broadening of the tan δ peak compared to the unsaturated polymers. Moreover, the temperature of this relaxation is shifted to higher temperatures by approximately 10°C in the hydrogenated series. This effect may be attributed to the presence of soft segment cyrstallinity in the hydrogenated polyurethanes. The soft segment crystallinity acts to increase the temperature of α relaxation and to change its shape. Such effects are also observed in other semicrystalline polymers such as polyethylene, polypropylene and poly-(ethylene terephthalate) (22-23). Soft segment crystallization and melting in these hydrogenated polymers were also observed in thermal studies by Schneider (24).

No conclusive evidence of a hard segment glass transition, which was found to occur between 30 and 100°C by DSC determination (24), is observable in the various dynamic mechanical relaxation measurements of both hydrogenated and unsaturated polymers. However, increasing the hard segment content increases the softening point presumably because of an increase in the hard segment sequence lengths.

3. Stress-Strain Measurements

The results of tensile tests performed at room temperature on films of hydrogenated and unsaturated polyurethanes are shown in Figure 8 and summarized in Table 1. In both series, as the percentage of hard segment increases, several systematic changes occur in the tensile properties. First, the initial modulus (slope of stress-strain curve) increases, indicating the greater rigidity imposed by the hard segment. The stress level during extension also increases with hard segment content again showing the effects of the less mobile hard segment domains which have difficulty sliding past one another. As expected, the ultimate elongation values for the two series of polymers decreases with increasing weight fraction of hard segment.

With the exception of sample 51, the initial modulus and stress level at break was higher in the hydrogenated samples than in the unsaturated ones. The ultimate elongations were also significantly higher. The two concurrent effects give rise to an increase in the toughness of the material, as determined by the areas under the curves.

Cyclic Instron tests were also performed on these samples and the results are shown in Figure 9. Readily apparent are two characteristics of stress softening. First, upon subsequent straining, lower stress levels are observed at all extensions lower than the maximum previously applied, and second, at strain levels higher than those previously reached, the stress levels are apparently unaffected by prestraining. Both the hydrogenated and

unsaturated materials behave similarly in this respect, the only noticeable difference was that HY-51 shows more permanent set than R-51. This stress-softening behavior is characteristic of phase separated materials and several interpretations of the phenomena are cited, including disruption of the polymer structure and of the reinforcing mechanism, chain slippage and chain breakage (21).

D. Summary

Dynamic mechanical relaxation measurements on several polybutadiene containing polyurethanes and their hydrogenated derivatives have revealed certain effects of composition and structure on transition phenomena. Both series displayed a low temperature and relatively composition insensitive relaxation associated with the glass transition temperature of the soft segment as well as modulus enhancement at temperatures above this relaxation. Although a hard segment Tg could not be clearly defined by the dynamic mechanical technique, thermal studies identified higher temperature relaxations occurring around 70°C which are associated with the hard segment. Our results suggest that the soft segment phase in these polyurethanes is relatively free of intermixed hard segments. Moreover, IR analysis indicates that most (90%) N-H bonding resides within the hard segments.

It is reasonable to assume that chemical modification of the polybutadiene segments by hydrogenation of the precursor prepolymer will lead to changes in the morphology and microstructure present in these polymers. IR analysis indicates preferential hydrogenation of the 1,2 vinyl and cis double bonds within the soft butadiene segments. In addition, bands were found at 720 cm^{-1} and 729 cm^{-1}, which can be assigned to amorphous polyethylene and two components of the crystal field splitting of the CH_2 rocking motion. These results, together with the broad melting behavior observed above the soft segment Tg in DSC scans, lead us to conclude that hydrogenation results in crystallinity within the soft segment.

The soft segment crystallinity acts to increase the temperature of the α relaxation and change its shape. Further, the presence of crystallites in the soft segment of the hydrogenated urethane polymers results in the enhancement of the stress values at a given strain due to these regions acting as tie-points.

II. A DYNAMIC MECHANICAL STUDY OF THE CURING REACTION OF AN EPOXY RESIN

A. Introduction

The work described herin represents an extension of the previous dynamic spring analysis, DSA, study of the curing of two epoxy resins (25,26) to a third epoxy resin. The current one consists of tetraglycidyl 4,4'-diaminodiphenyl methane epoxide (TGDDM) and the curing agent, diaminodiphenyl sulfone (DDS). An activation energy for the curing process was calculated from the loss tangent spectra. The loss tangent, when plotted versus time at constant temperature, displayed two peaks instead of the single anticipated dispersion; this broadening or splitting into two peaks was observed at all four of the temperatures used in the study.

B. Experimental

1. Samples

The formulation containing the TGDDM (A) and DDS (B) is known commercially as 5208 Narmco. The sample used in this study was supplied by the Polymer and Chemistry Division of the Army Materials and Mechanics Research Center at Watertown, MA.

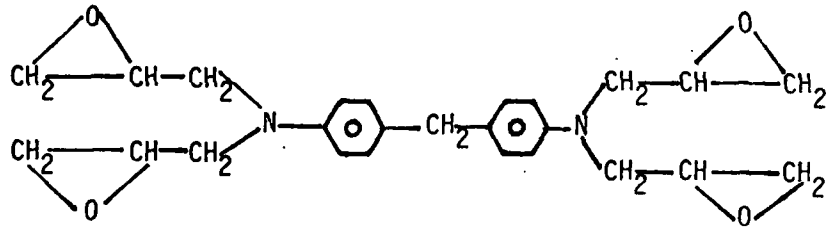

(A)

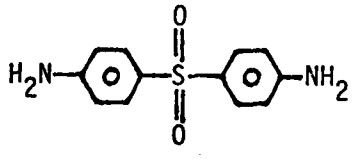

(B)

2. Measurements

The curing reaction was followed by the technique of dynamic spring analysis (DSA) in conjunction with the Rheovibron DDV-IIB dynamic viscoelastometer, as described previously (26, 27). A spring, 3.3. mm in outer diameter, of .30 mm diameter steel wire, twenty turns in length, was placed in the Rheovibron and stretched to achieve a pitch of .1 mm. The Rheovibron temperature chamber was then brought to a constant cure temperature and the sample applied with a hypodermic syringe as a 50 percent by weight clear solution in methylene chloride. The viscoelastic response was followed at four different frequencies in a dry nitrogen atmosphere as a function of time

from the moment of sample application. About 15 mg of epoxy sample was required for each isothermal cure.

C. Results and Discussion

As noted previously (26), the usefulness of the DSA technique in following epoxy curing systems stems from the fact that a relative maximum is produced in the composite loss tangent, tan δ, versus time curve when the viscosity of the resin reaches a predetermined value. Figure 10 shows a plot of tan δ versus the natural logarithm of time (seconds) for an isothermal cure at 147°C; at 110, 35, 11 and 3.5 Hz. At each frequency, a second peak occurring at longer times is apparent in addition to the viscosity-related dispersion. Both peaks become smaller and shift to longer times as ω decreases; the separation between the two peaks also increases with decreasing ω. Figure 11 shows a plot of tan δ versus ln (t) at 3.5 Hz for four different curing temperatures. As expected, the highest temperature results in the earliest onset of the loss peak associated with the change in resin viscosity. Note that the separation between the two peaks increases at the higher temperature.

In a previous study (28) in which a series of polystyrenes of varying molecular weights was characterized by DSA, the theoretical basis for understanding the viscosity-related peak was established. The study also showed that the Tg or vitrification process is not detectable by DSA. Figure 12 displays plots of the composite tan δ versus temperature for five polystyrene samples whose molecular weights vary from 2,000 to 92,500. At Mw= 37,000, a distinct shoulder appears on the central peak; at Mw=92,5000, the broadening is even more pronounced. Because 37,000 is associated with the minimum chain length needed for entanglement coupling, it was suggested that the appearance of a second peak well beyond the Tg was due to the relaxation of entanglements.

Here, we believe that the second peak observed in the curing studies is related to the presence of polymer chains of sufficient length to permit entanglement coupling. The fact that only one dispersion was observed in the curing study reported previously (25) indicates that the chemical reaction beyond the point of the observed maximum may be sufficiently rapid so as to reach the glassy state before a second peak can be witnessed. It should be noted that the presence of only one peak in a high molecular weight system is an anomaly rather than the rule.

To better characterize the secondary relaxation, the storage, Mp' and loss, Mp", moduli of the polymer were extracted from the complex modulus of the composite, Mc*. It was, therefore, necessary to assume a particular model such as the parallel one, whose defining equation is:

$$Mc^* = Mp^* + Ms^* \qquad (1)$$

where Ms*, the spring modulus, is assumed to be Hookean, i.e. Ms*=Ms'; Ms"=0. Ms' is also assumed to be independent of temperature in the region of operation. Figure 13 displays plots of Mp' and Mp", measured at 3.5 and 110 Hz, versus ln(t) for the resin cured at 147°C. If the resin behaved as

a simple Newtonian liquid at all times, $Mp''=\eta\omega$ and $Mp'=0$; where η is the viscosity and ω is the angular frequency, $2\pi f$. In this mode of analysis, the long-time relaxation is dominant and the viscosity-related one appears as an unresolved shoulder on the left side of the large peak. Because of the unresolved nature of these two dispersions, no attempt was made to extract additional information from the Mp' and Mp" versus ln(t) plots.

Because the elapsed time to the composite tan δ maximum, t_{max}, is merely the time required to attain a specific viscosity (at constant ω), t_{max} can be used as a convenient measure of the rate of reaction at each temperature and for each frequency. Since the velocity constant, K, for a chemical reaction is inversely proportional to t_{max}, is independent of reaction order, and varies with temperature according to:

$$\ln(K) = -\frac{Ha}{RT} + C \qquad (2)$$

the activation energy, Ha, of the reaction can be determined from the slope of a plot of $\ln(t_{max})$ versus 1/T as in Figure 14. For each frequency, the data can be fit to a straight line. A linear least squares fit was used to determine Ha at each frequency; the results appear in Table 2. The slight frequency dependence of Ha is probably caused by the perturbation of the location of t_{max} by the proximity of the second peak. Since the peaks are better resolved at 3.5 Hz, the corresponding value of 15.8 kcal/mole is the most accurate of the four values given.

The same epoxy resin was studied by torsional braid analysis, TBA, (24); the curing times were found to be 60% shorter than the values reported here. The reason for this discrepancy is currently under investigation. The fact that DDS has a melting temperature of 162°C and could, therefore, form a solid dispersion after the methylene chloride has evaporated form the film may be relevant. The appearance of the second peak in DSA is consistent with an overall slower reaction mechanism in the epoxy resin cure studied here.

In hope of obtaining additional information about the kinetics of the curing process, the logarithmic viscosity was plotted versus reaction time for each of the isothermal cures, as in reference (25); the results appear in Figure 15. The complex nature of the curing process is demonstrated by the fact that a nonlinear plot is obtained; a logarithmic variation of viscosity with time would indicate a pseudo first order reaction. It is not possible to obtain quantitative information from such plots without additional experimental viscosity measurements and the introduction of a highly speculative model as to the chemical species present in the resin at all of the times under study.

D. Summary

The work described demonstrates both the advantages and disadvantages of the DSA technique for studying the curing of epoxy resins. The technique is well suited to the determination of the onset of gelation under isothermal curing conditions; however, the method requires additional refinement before the later stages of the reaction can be examined in a quantitative fashion.

The average value of the activation energy for the onset of gelation in the resin here is 15.2 kcal/mole. The loss tangent maxima appearing first in an isothermal cure result from the rapid increase in resin viscosity; the temporal location of the maximum depends on the frequency at which the experiment is conducted. In order to better characterize the kinetics of the curing process, it will be necessary to use appropriate analytical techniques to monitor the chemical species and their respective concentrations present in the resin at all times.

III. REFERENCES

1. C. Arnold, Jr., J. Elastomers Plastics, 6, 238 (1974).
2. R.D. Elmore, Use of EN-7 to Encapsulate Analyzer Assemblies, [illegible]9183, Sept. 1974.
3. G.B. Wood, Evaluation of Conformal Coatings of Microelectronic Circuitry in Fuse Applications, MDL-TR-1777, March 1977.
4. J.A. Verdol, P.W. Ryan, D.J. Carrow and K.L. Kund, Rubber Age, 57 (1966).
5. Ibid, 98, 6 (1969).
6. D.M. French, Rubber Chem. Technol., 42, 71 (1969).
7. N.S. Schneider and C.S. Park Sung, Polym. Eng. Sci., 17, [illegible]
8. J. Strassburger and I.T. Smith, Appl. Spectros., 33, 283 [illegible]
9. S.L. Hsu, W.H. Moore and S. Krimm, J. Appl. Phys., 46, 4136 [illegible]
10. J.L. Binder, J. Polym. Sci., A3, 1587 (1965).
11. L.A. Mango and R.W. Lenz, Makromol. Chem., 163, 13 (1973).
12. R.G. Snyder and J.H. Schachtschneider, Spectrochim. Acta [illegible] (1963).
13. R.G. Snyder, J. Chem. Phys., 47, 1316 (1967).
14. R.G. Snyder, J. Mol. Spectrosc., 7, 116 (1961).
15. R.S. Stein and G.B.B.M. Sutherland, J. Chem. Phys., [illegible]
16. R.W. Seymour, G.M. Estes and S.L. Cooper, Macromol., 3, 579 [illegible]
17. W.J. MacKnight and M. Yang, J. Polym. Sci., C, 42, 817 (1973).
18. T. Tanaka, T. Yokoyama and Y. Yamaguchi, J. Polym. Sci. A-1, 6, 2153 (1968).
19. C.S. Park Sung and N.S. Schneider, Macromol., 10, 452 (1977).
20. V.W. Srichatrapimuk and S.L. Cooper, J. Macromol. Sci. Phys., B15, 267 (1978).
21. G.M. Estes, S.L. Cooper and A.V. Tobolsky, J. Macromol. Sci. Rev. Macromol. Chem., C4, 313 (1970).

22. K.H. Illers, Kolloid Z.Z. Polym., 250, 426 (1972).

23. T.R. Earnest, Jr. and W.J. MacKnight, Macromol., 10, 206 (1977).

24. N.S. Schneider, Army Materials and Mechanics Research Center (unpublished).

25. Final Report - U.S. Army Contract DAAG-46-77-C-0031 (1978).

26. G.S. Senich, W.J. MacKnight and N.S. Schneider, Polym. Eng. Sci., 19, 313 (1979).

27. G.A. Senich and W.J. MacKnight, J. Appl. Polym. Sci., 22, 2633 (1978).

28. R.M. Neumann, G.A. Senich and W.J. MacKnight, Polym. Eng. Sci., 18, 624 (1978).

TABLE 1

Characterization Data for HTPBD-Containing
Polyurethanes and Their Hydrogenated Derivatives

	PU-Unsaturated			PU-Hydrogenated		
Sample	R-50	R-51	R-52	HY-50	HY-51	HY-52
Composition PBD/TDI/BDO	1.0/4.2/3.1	1.0/6.5/5.3	1.0/8.4/6.9	1.0/4.1/2.9	1.0/6.4/5.2	1.0/8.3/7.3
Wt. % Hard Segment	27.2	37.9	43.8	26.3	36.5	43.4
Dynamic (11Hz) Glass Transition						
Temperatures, °C						
From E''_{max}	-74.4	-73.5	-73.7	-69.5	-69.5	-68.8
From tan δ_{max}	-64.8	-63.2	-64.8	-54.5	-53.1	-53.7
Magnitude tan δ_{max}	.700	.548	.410	.405	.380	.340
T_{max} (°C) for E'	30	61	107	30	66	103
Polymer Physical Properties						
Tensile stress (σ_B), dyne/cm^2 x 10^{-7}	3.9	9.6	9.7	8.4	9.3	13.2
Ultimate elongation, %	340	230	150	410	380	260

TABLE 2

Narmco 5208 Resin

Chemical Activation Energy from DSA

Frequency, Hz	H_a, kcal/mole
110	14.4
35	15.1
11	15.4
3.5	15.8
Avg.	15.2

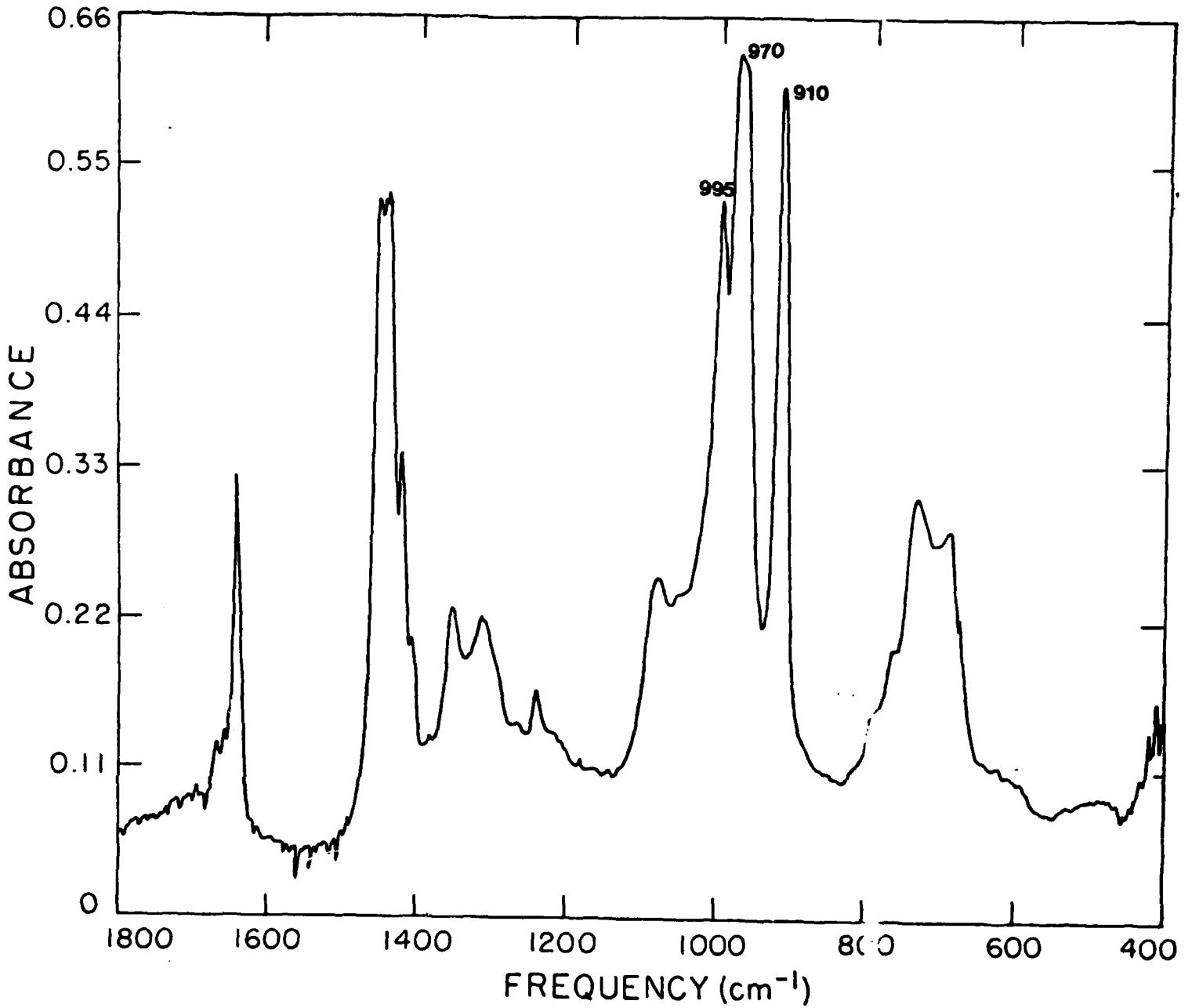
0.66
0.55
0.44
0.33
0.22
0.11
0
ABSORBANCE
970
910
995
1800
1600
1400
1200
1000
800
600
400
FREQUENCY (cm⁻¹)

Fig 1

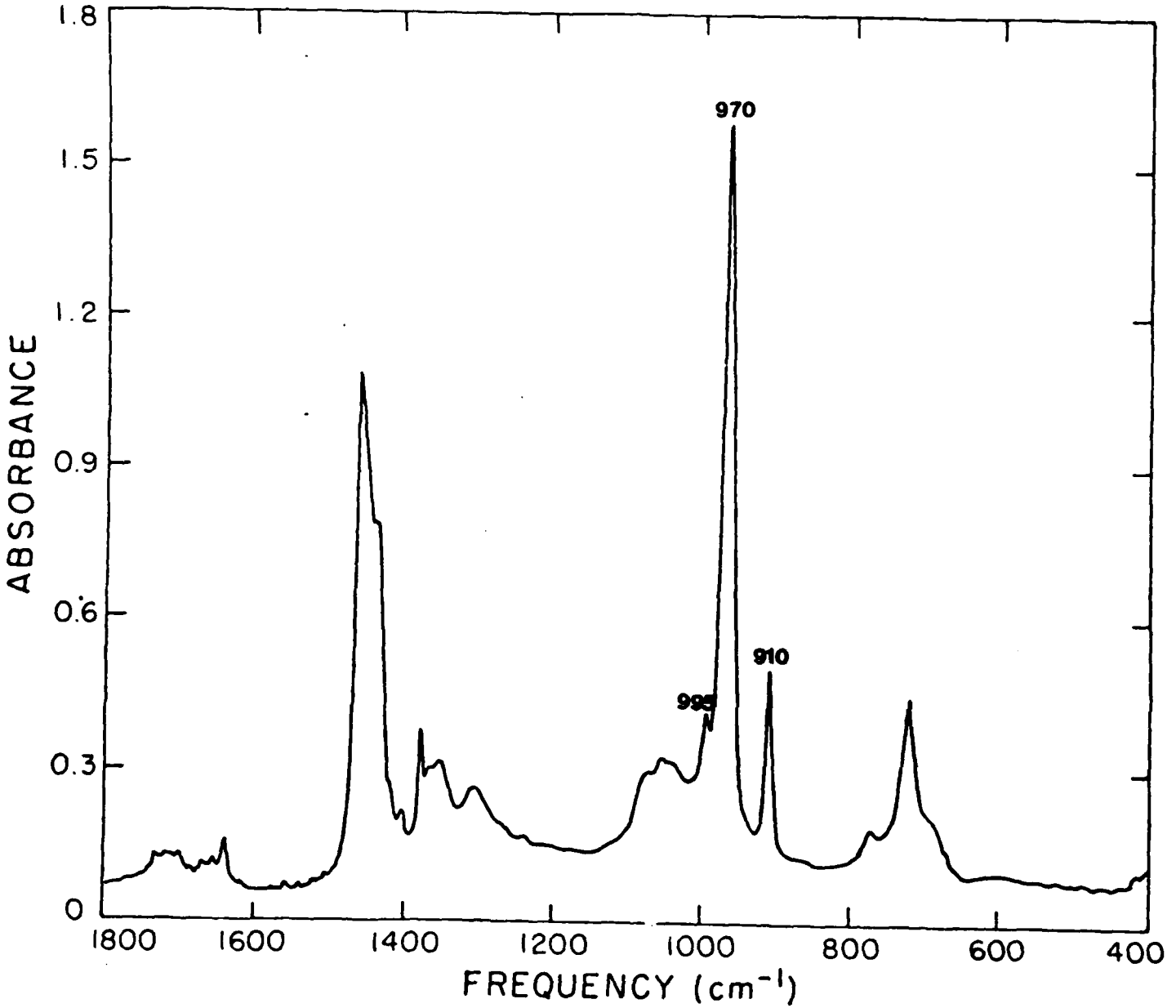
1.8
1.5
1.2
0.9
0.6
0.3
0
ABSORBANCE
970
910
995
1800
1600
1400
1200
1000
800
600
400
FREQUENCY (cm⁻¹)

Fig 2a

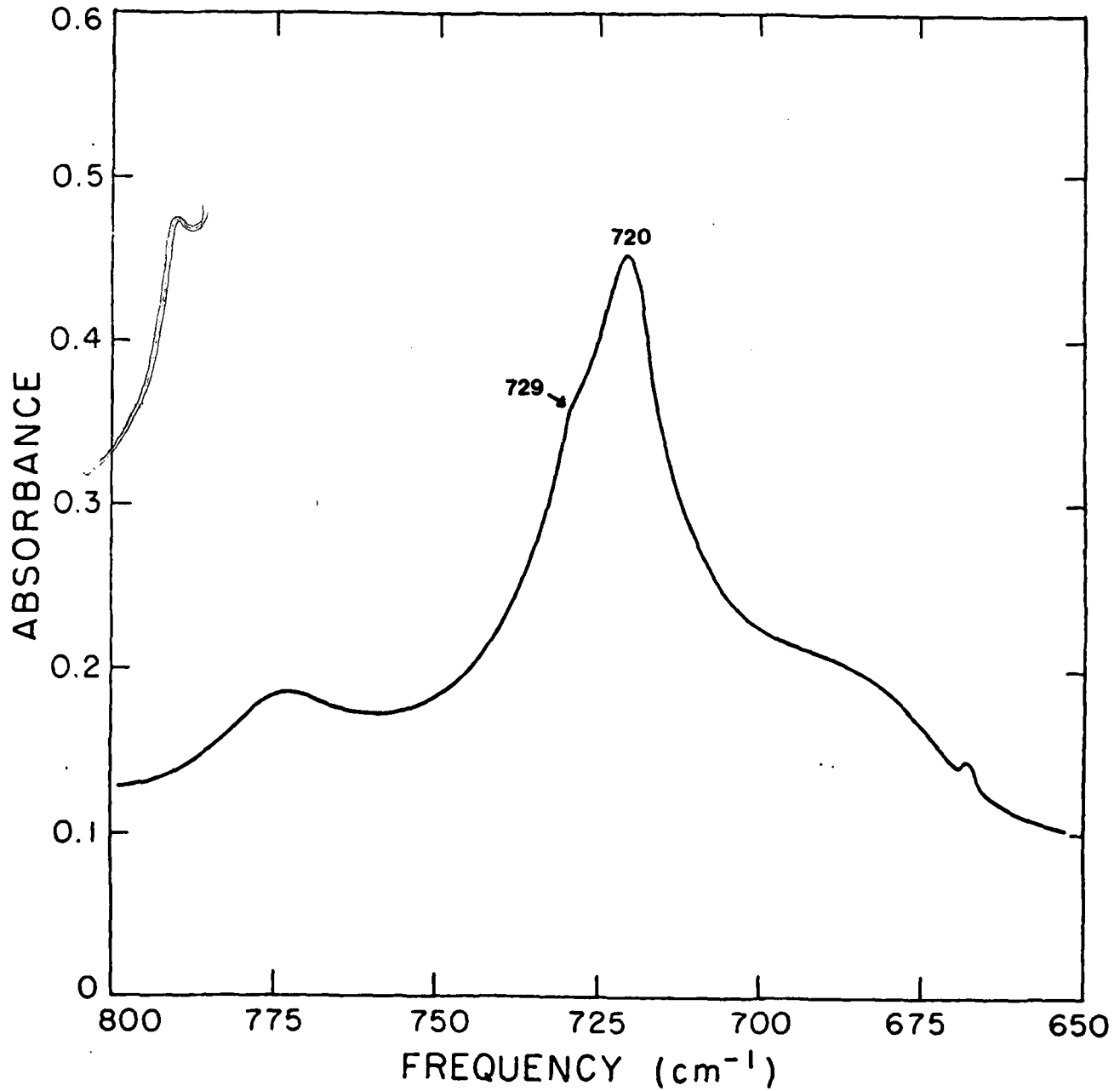
0.6
0.5
0.4
0.3
0.2
0.1
0
ABSORBANCE
720
729
800
775
750
725
700
675
650
FREQUENCY (cm⁻¹)

Fig 26

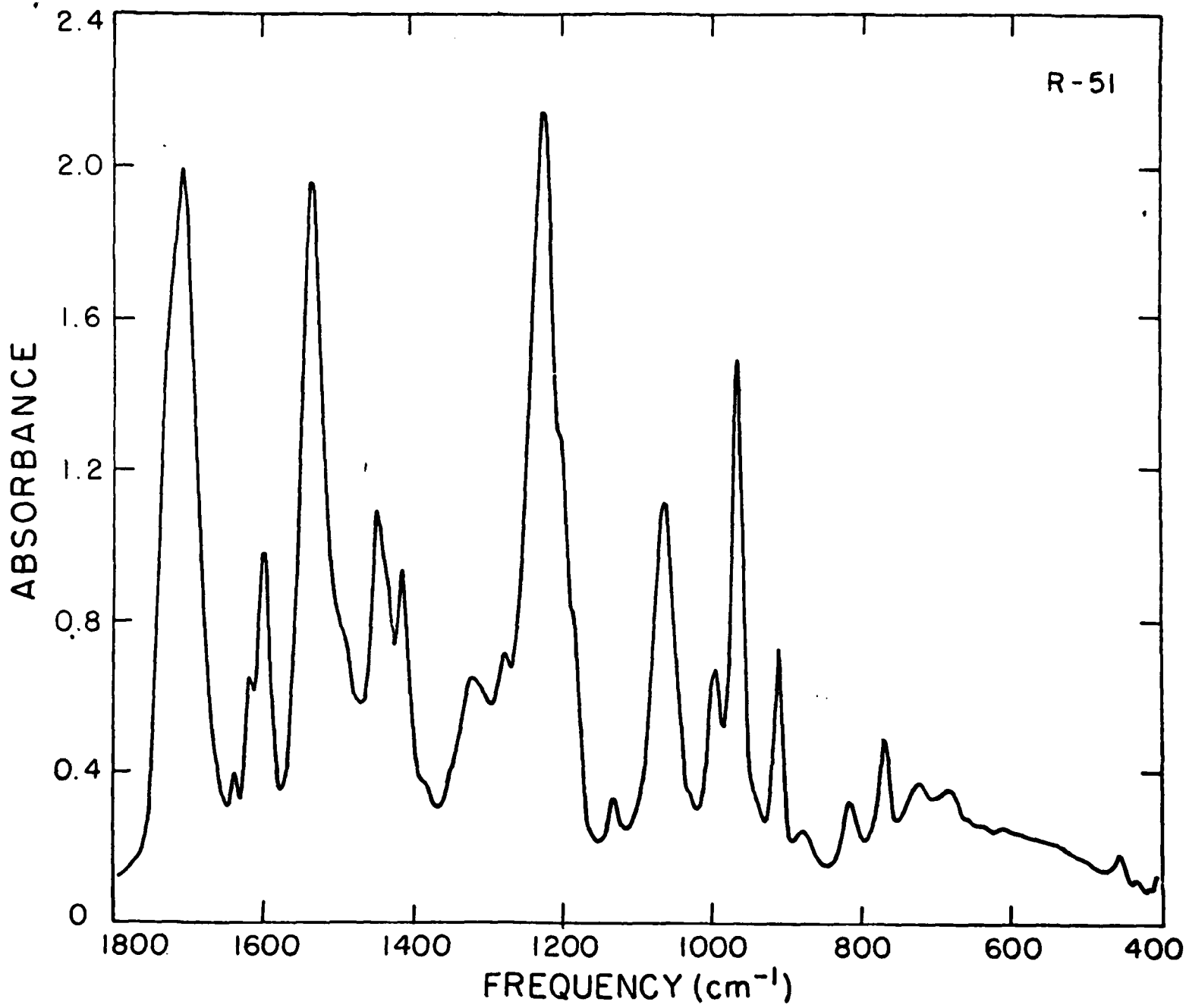
R-51
ABSORBANCE
2.4
2.0
1.6
1.2
0.8
0.4
0
1800
1600
1400
1200
1000
800
600
400
FREQUENCY (cm⁻¹)

Fig 3

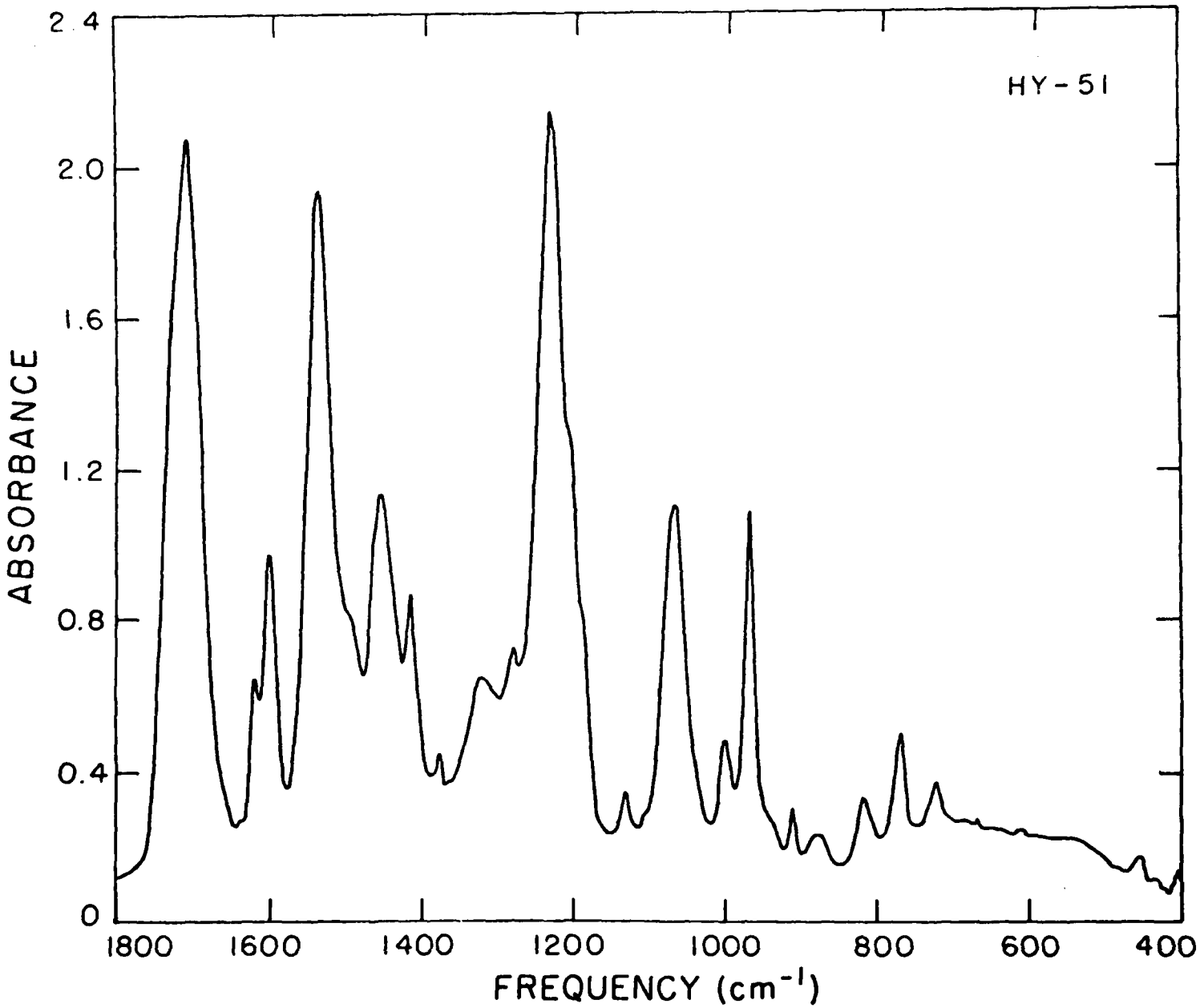
HY-51
ABSORBANCE
2.4
2.0
1.6
1.2
0.8
0.4
0
1800
1600
1400
1200
1000
800
600
400
FREQUENCY (cm⁻¹)

Fig 4.

HY-51

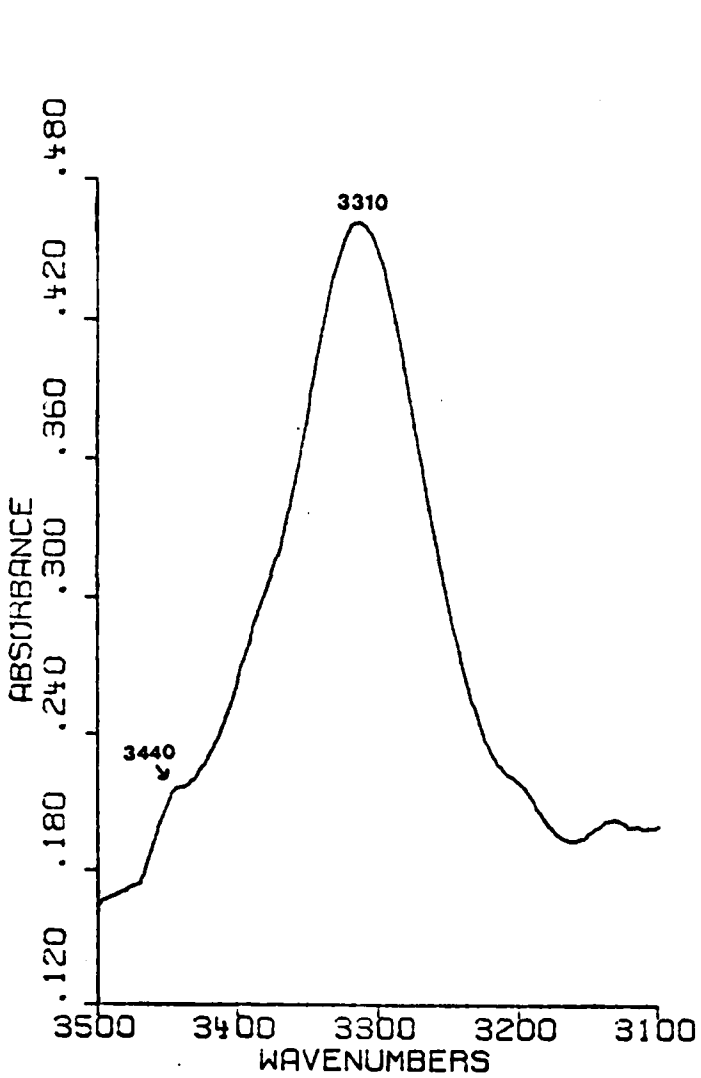
ABSORBANCE
.120
.180
.240
.300
.360
.420
.480
3310
3440
3500
3400
3300
3200
3100
WAVENUMBERS

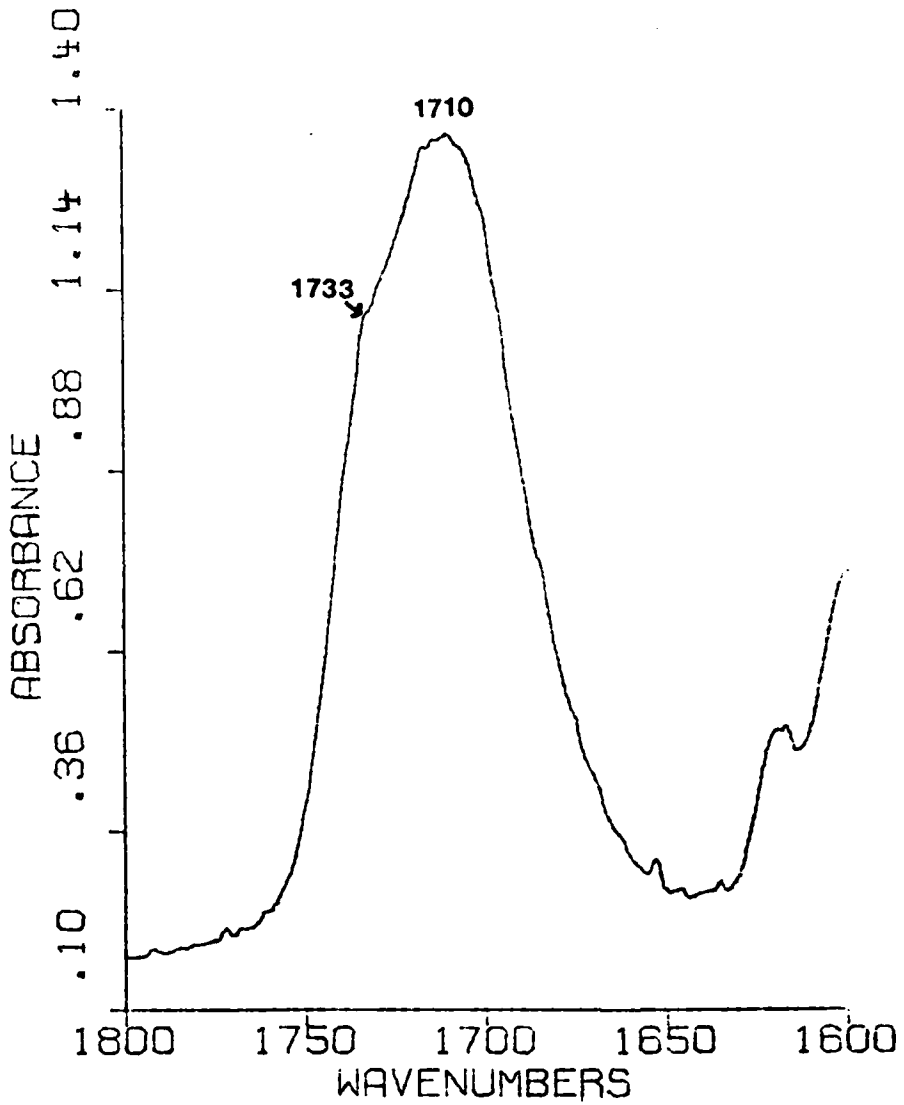
ABSORBANCE
.10
.36
.62
.88
1.14
1.40
1710
1733
1800
1750
1700
1650
1600
WAVENUMBERS

Fig 5

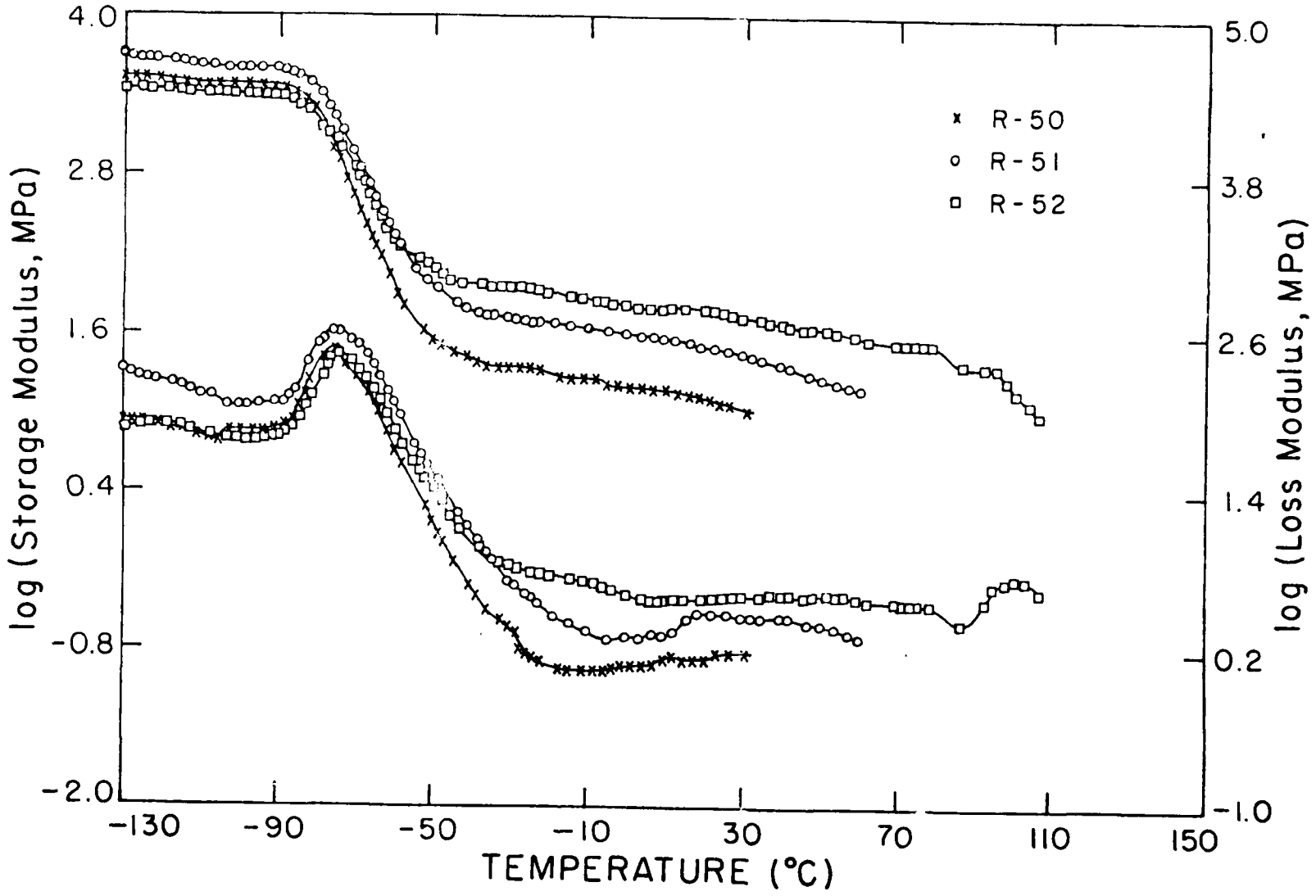
4.0
2.8
1.6
0.4
-0.8
-2.0
log (Storage Modulus, MPa)
5.0
3.8
2.6
1.4
0.2
-1.0
log (Loss Modulus, MPa)
R-50
R-51
R-52
-130
-90
-50
-10
30
70
110
150
TEMPERATURE (°C)

Fig 6a

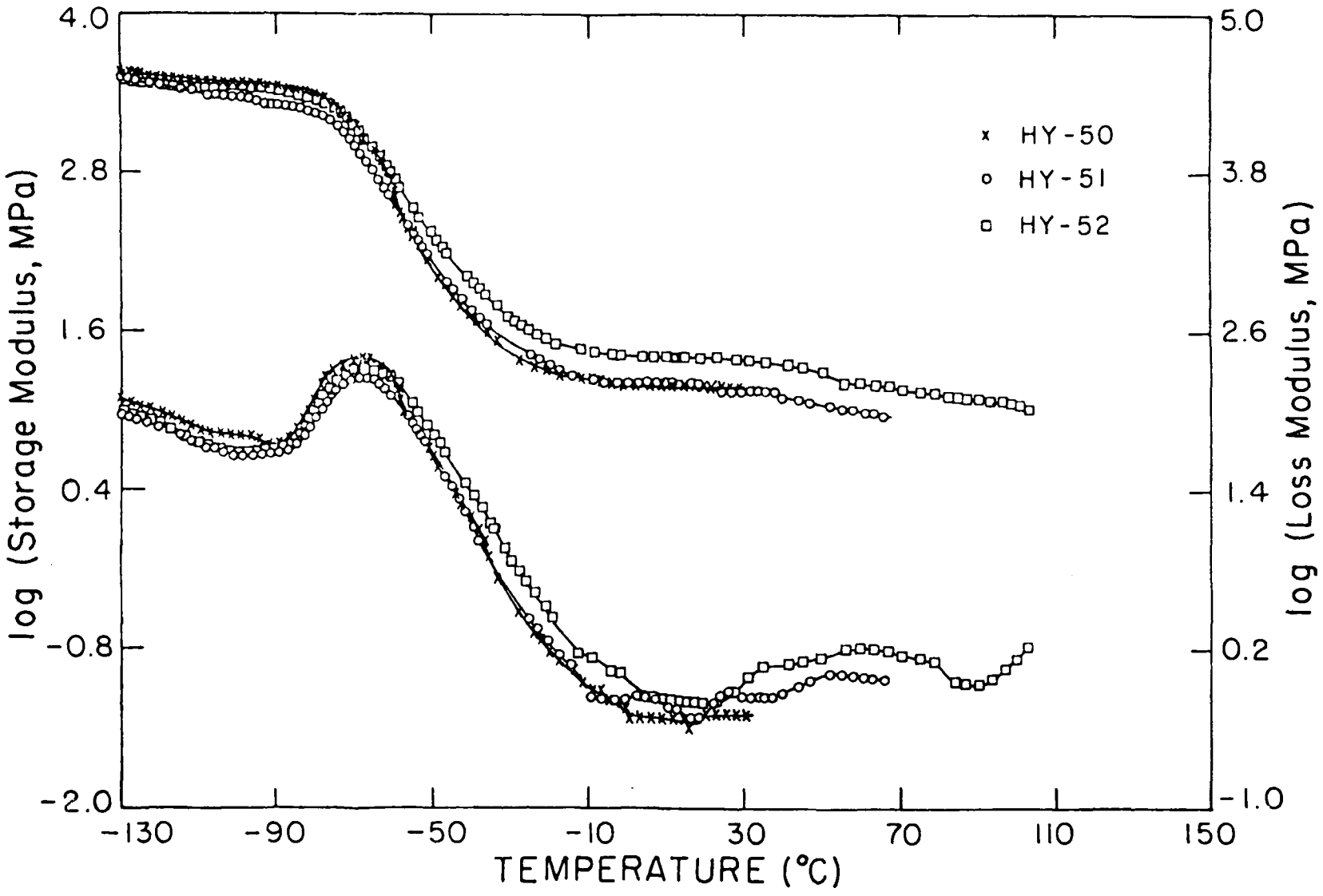
4.0
2.8
1.6
0.4
-0.8
-2.0
log (Storage Modulus, MPa)
5.0
3.8
2.6
1.4
0.2
-1.0
log (Loss Modulus, MPa)
HY-50
HY-51
HY-52
-130
-90
-50
-10
30
70
110
150
TEMPERATURE (°C)

Fig 66

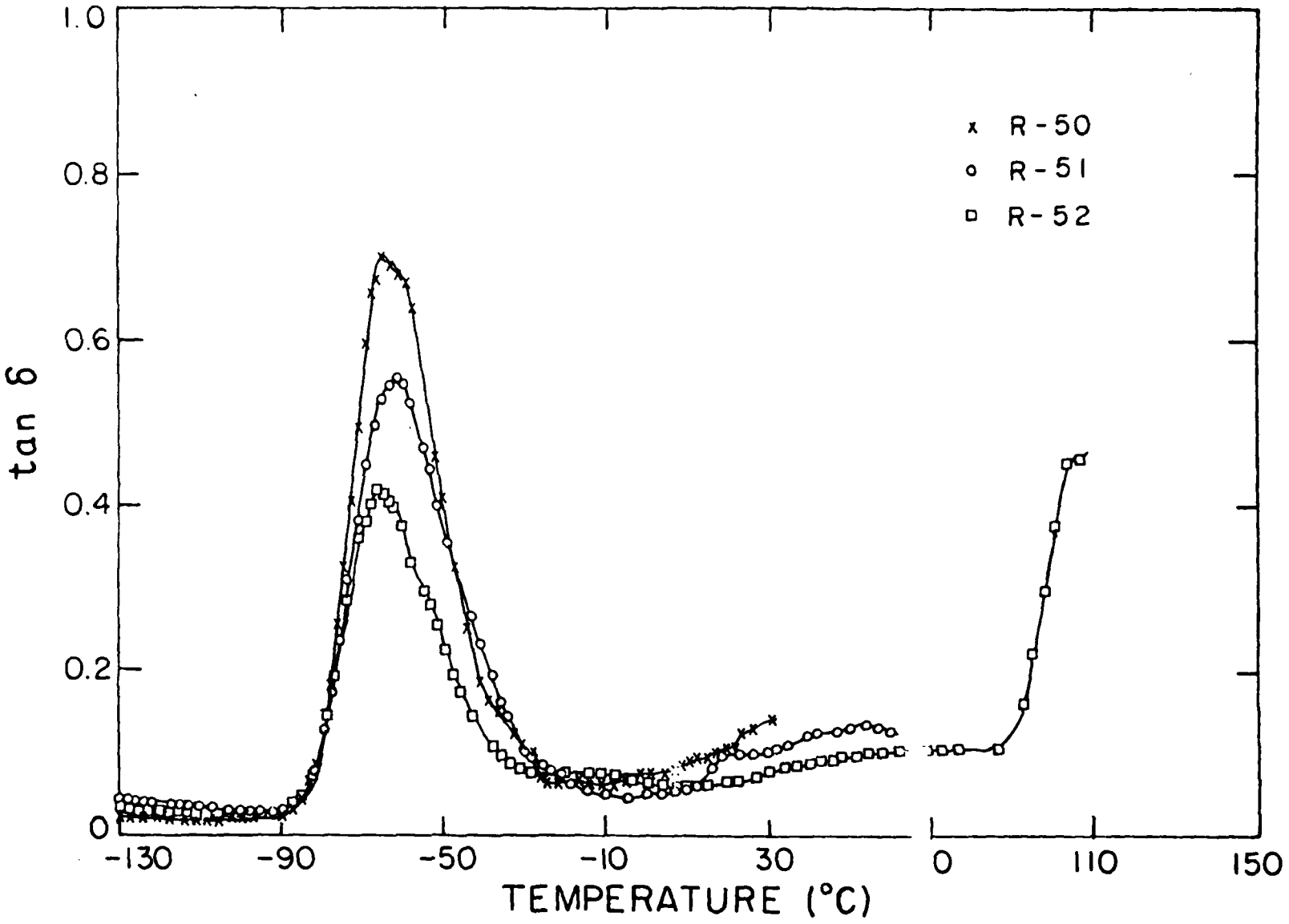
1.0
0.8
0.6
0.4
0.2
0
tan δ
R-50
R-51
R-52
-130
-90
-50
-10
30
0
110
150
TEMPERATURE (°C)

Fig 7a

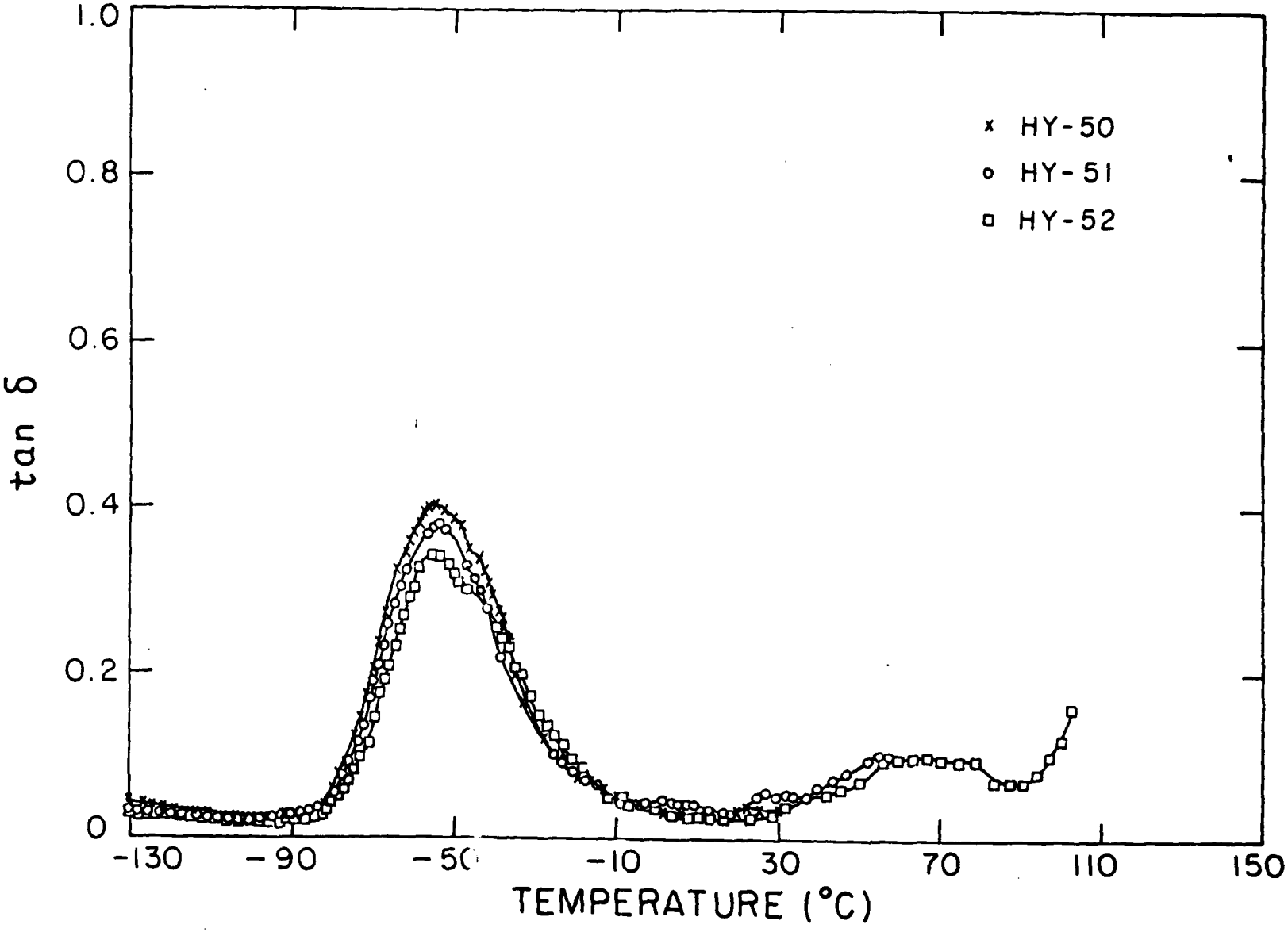
1.0
0.8
0.6
0.4
0.2
0
tan δ
HY-50
HY-51
HY-52
-130
-90
-50
-10
30
70
110
150
TEMPERATURE (°C)

Fig 76

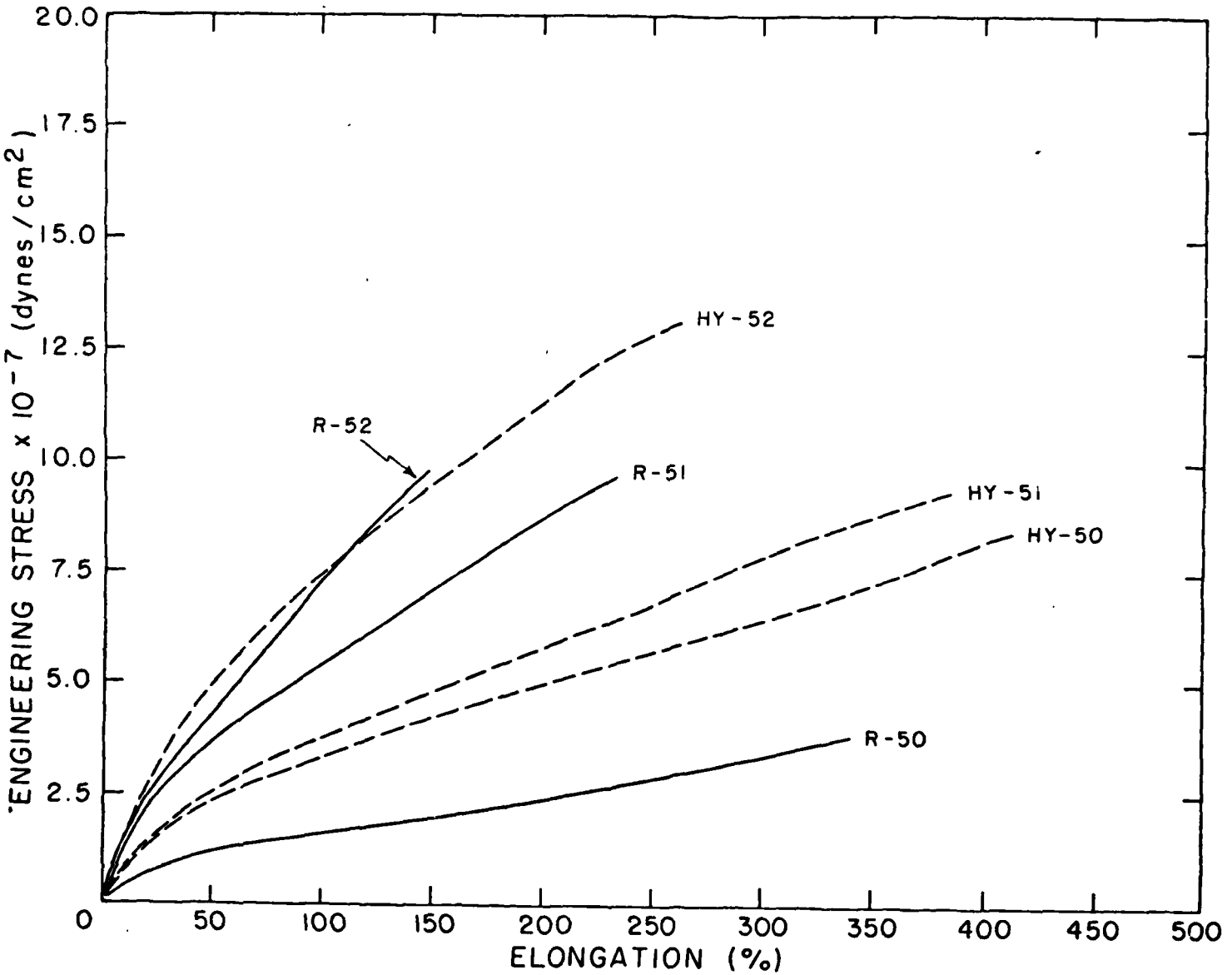
20.0
17.5
15.0
12.5
10.0
7.5
5.0
2.5
0
ENGINEERING STRESS x 10^{-7} (dynes/cm^2)
50
100
150
200
250
300
350
400
450
500
ELONGATION (%)
HY-52
R-52
R-51
HY-51
HY-50
R-50

Fig 8

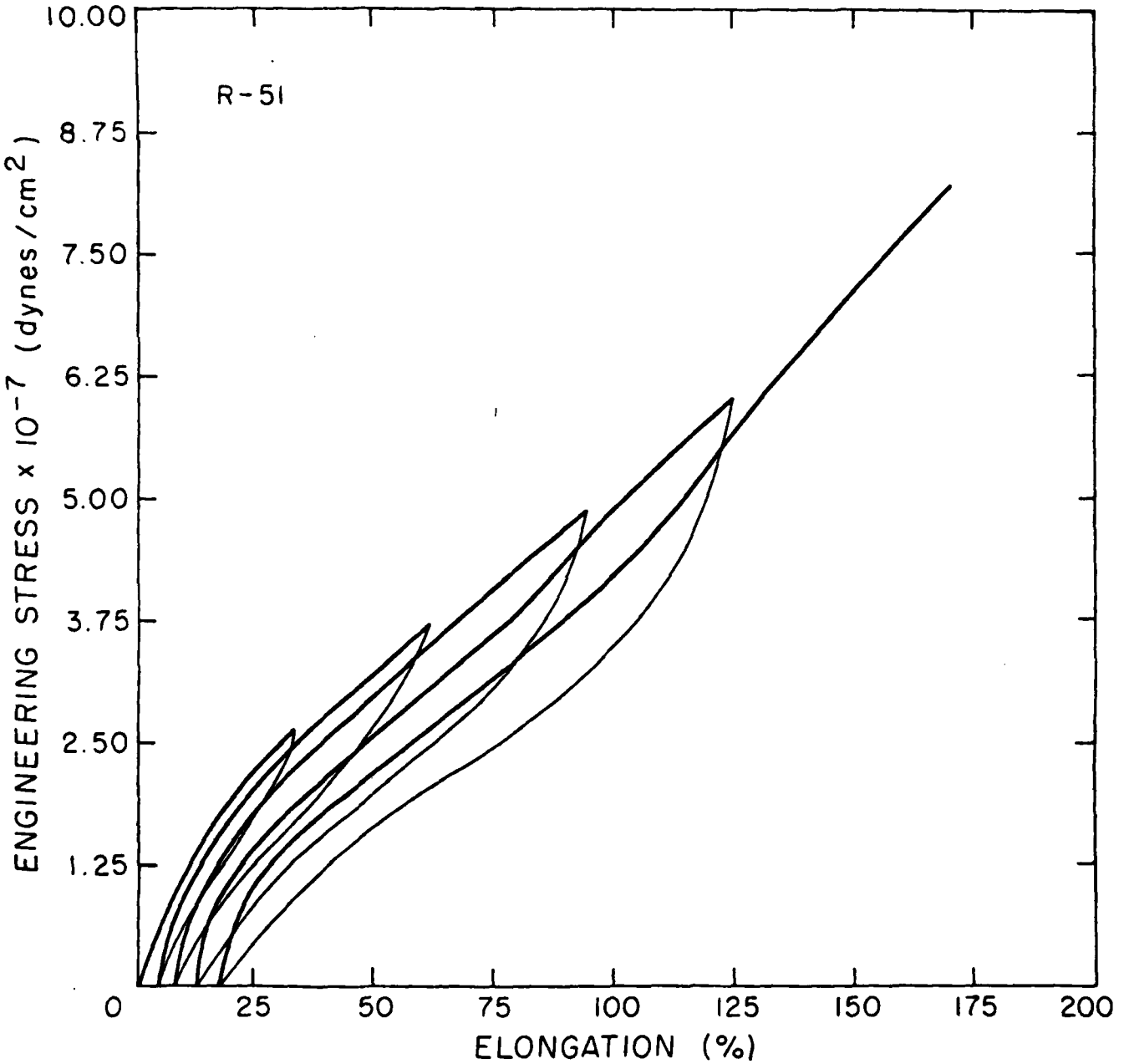
R-51
10.00
8.75
7.50
6.25
5.00
3.75
2.50
1.25
0
25
50
75
100
125
150
175
200
ENGINEERING STRESS x 10^{-7} (dynes/cm^2)
ELONGATION (%)

Fig 9a

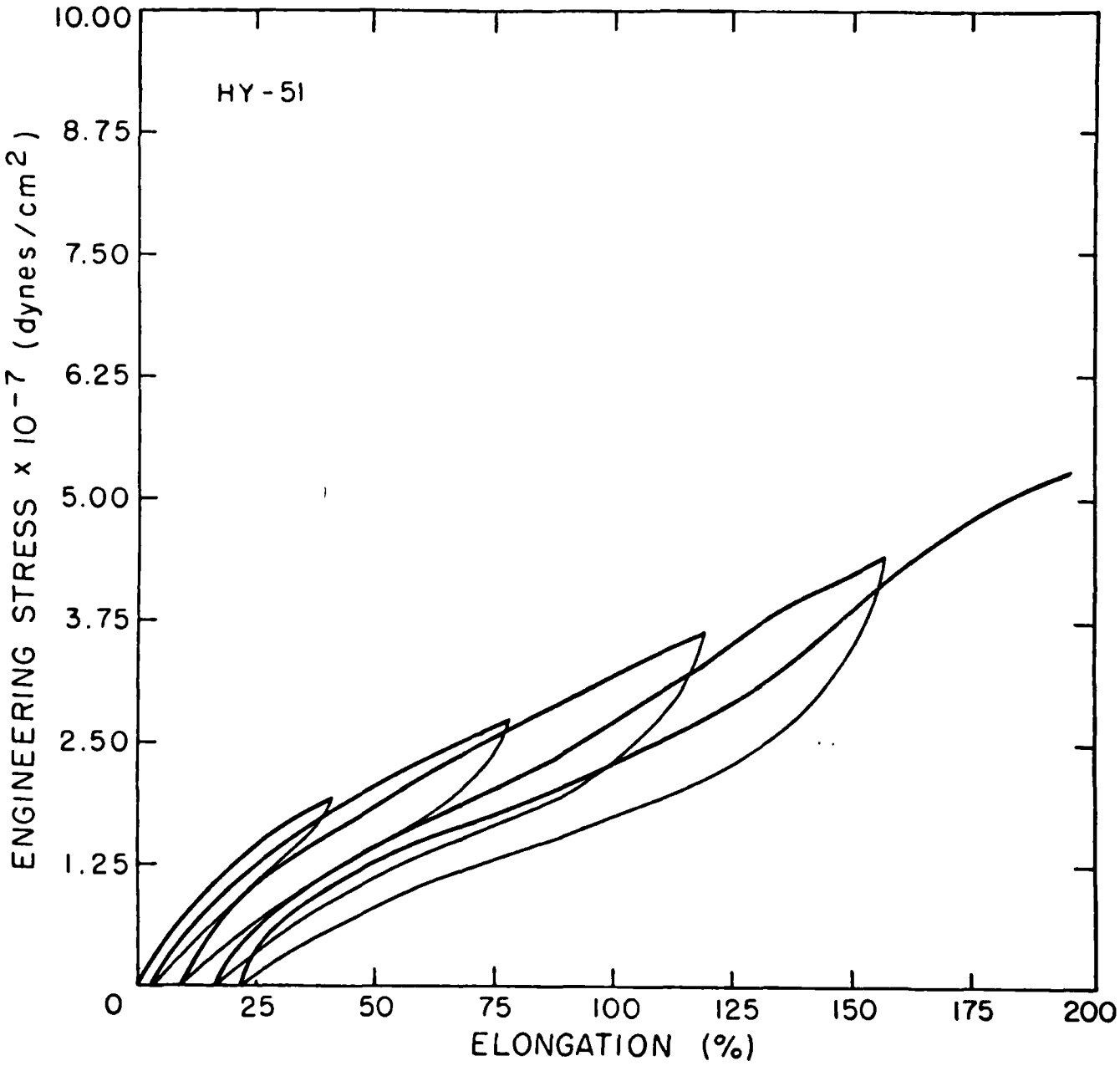
HY - 51
ENGINEERING STRESS x 10⁻⁷ (dynes/cm²)
10.00
8.75
7.50
6.25
5.00
3.75
2.50
1.25
0
25
50
75
100
125
150
175
200
ELONGATION (%)

Fig 96

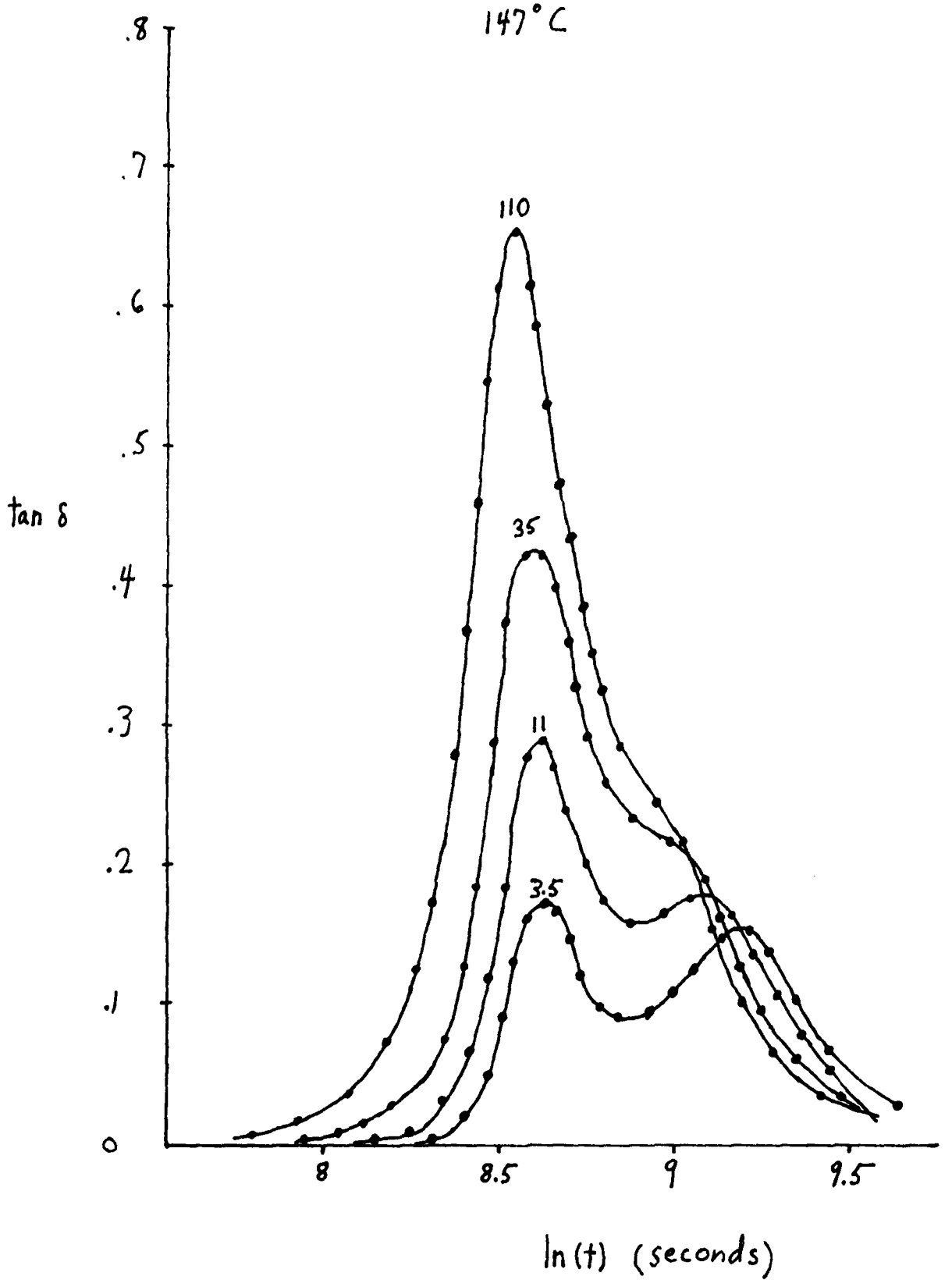

Fig 10

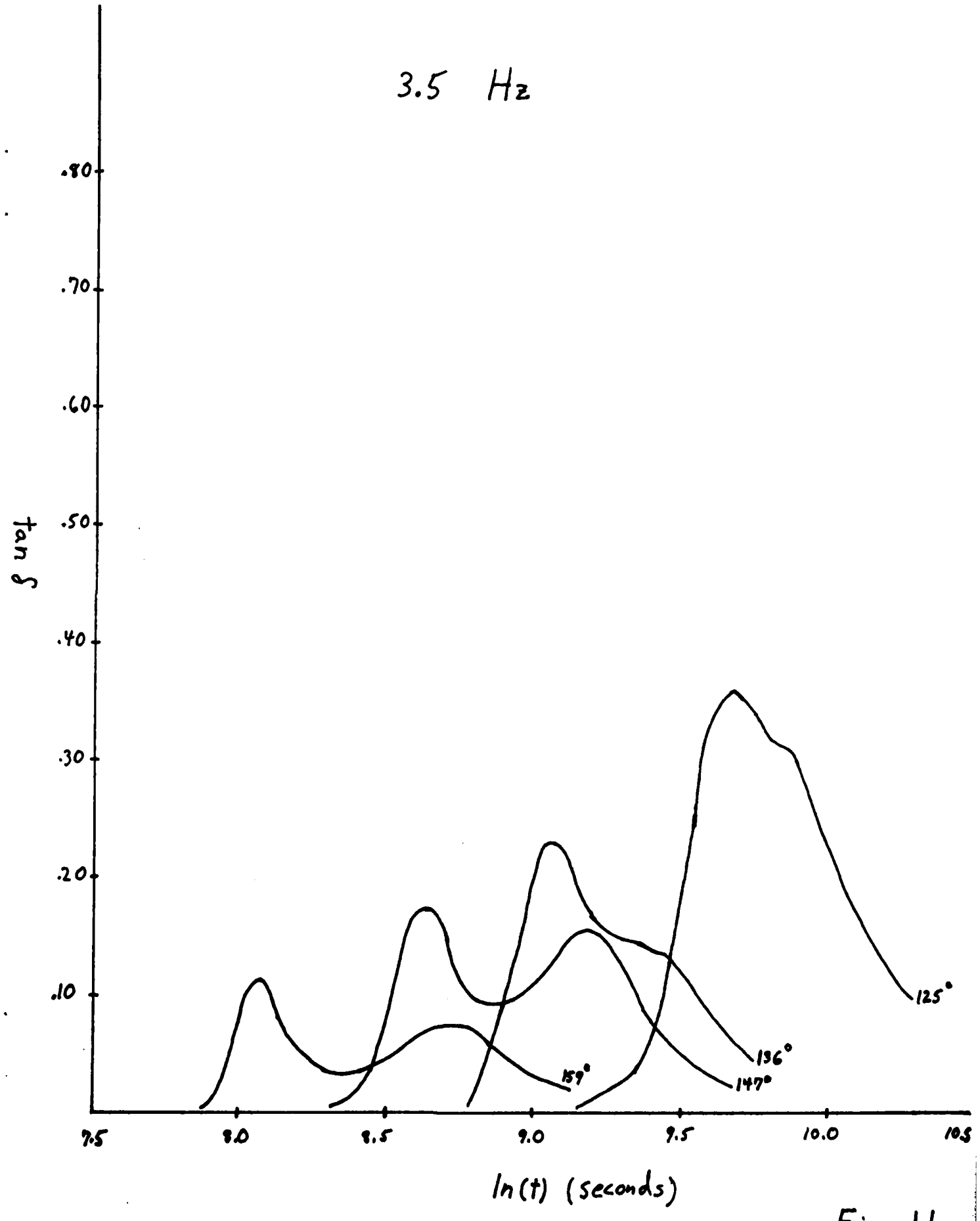
3.5 Hz
.80
.70
.60
.50
.40
.30
.20
.10
tan δ
7.5
8.0
8.5
9.0
9.5
10.0
10.5
ln(t) (seconds)
125°
136°
147°
159°

Fig 11

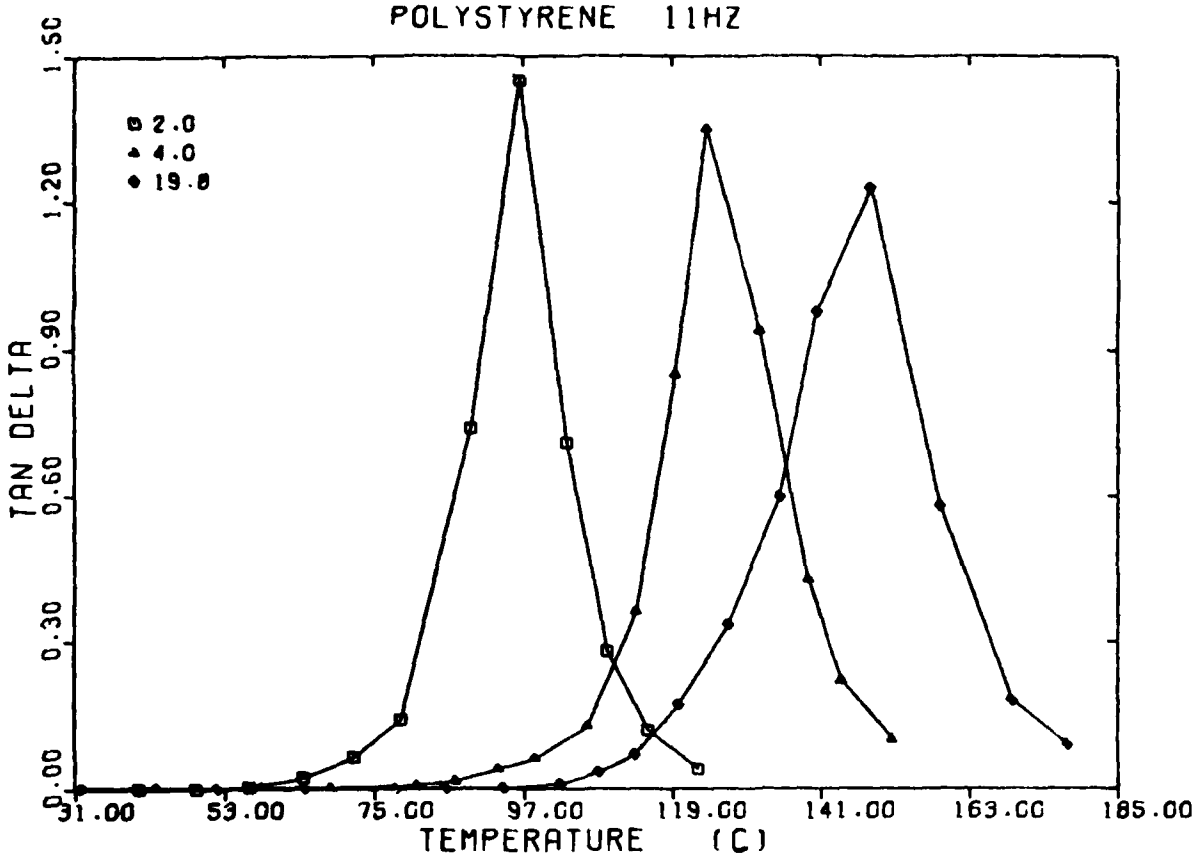
POLYSTYRENE 11HZ
2.0
4.0
19.8
TAN DELTA
0.00
0.30
0.60
0.90
1.20
1.50
31.00
53.00
75.00
97.00
119.00
141.00
163.00
185.00
TEMPERATURE (C)

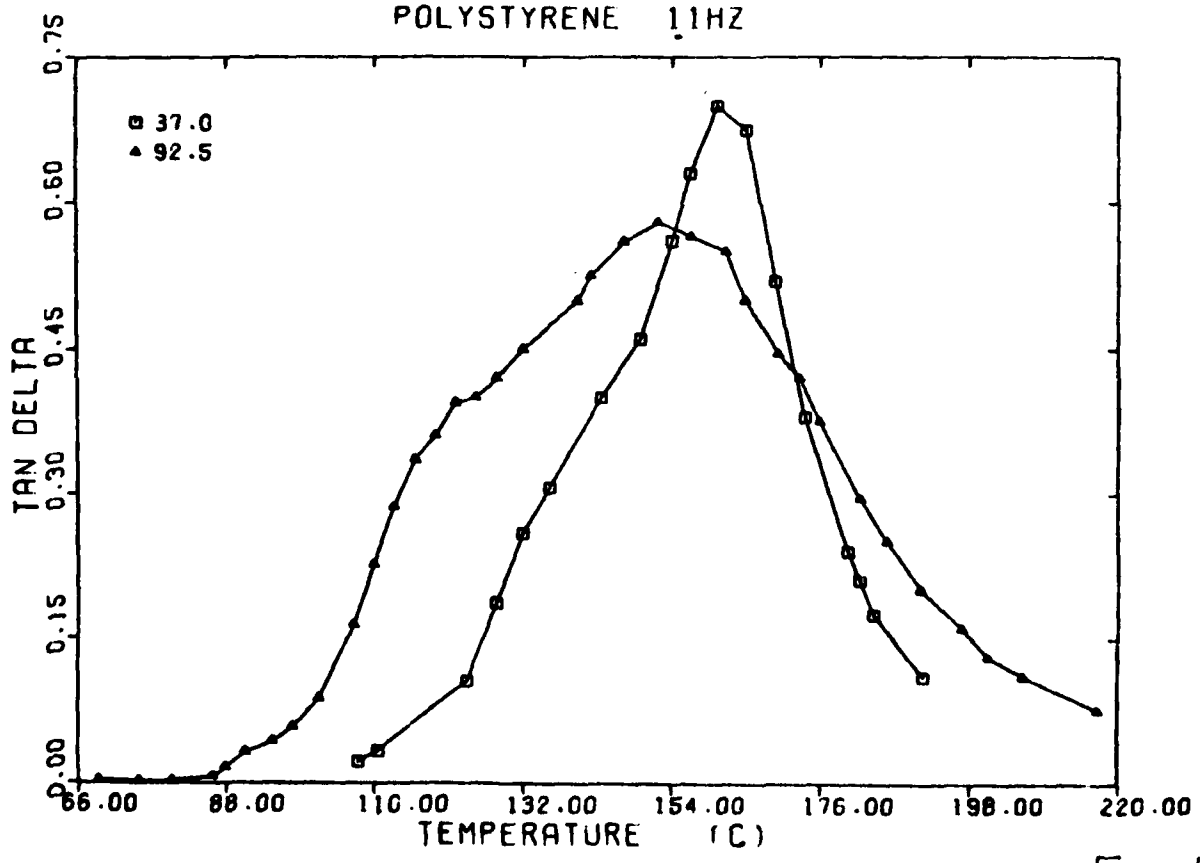
POLYSTYRENE 11HZ
37.0
92.5
TAN DELTA
0.00
0.15
0.30
0.45
0.60
0.75
66.00
88.00
110.00
132.00
154.00
176.00
198.00
220.00
TEMPERATURE (C)

Fig 12

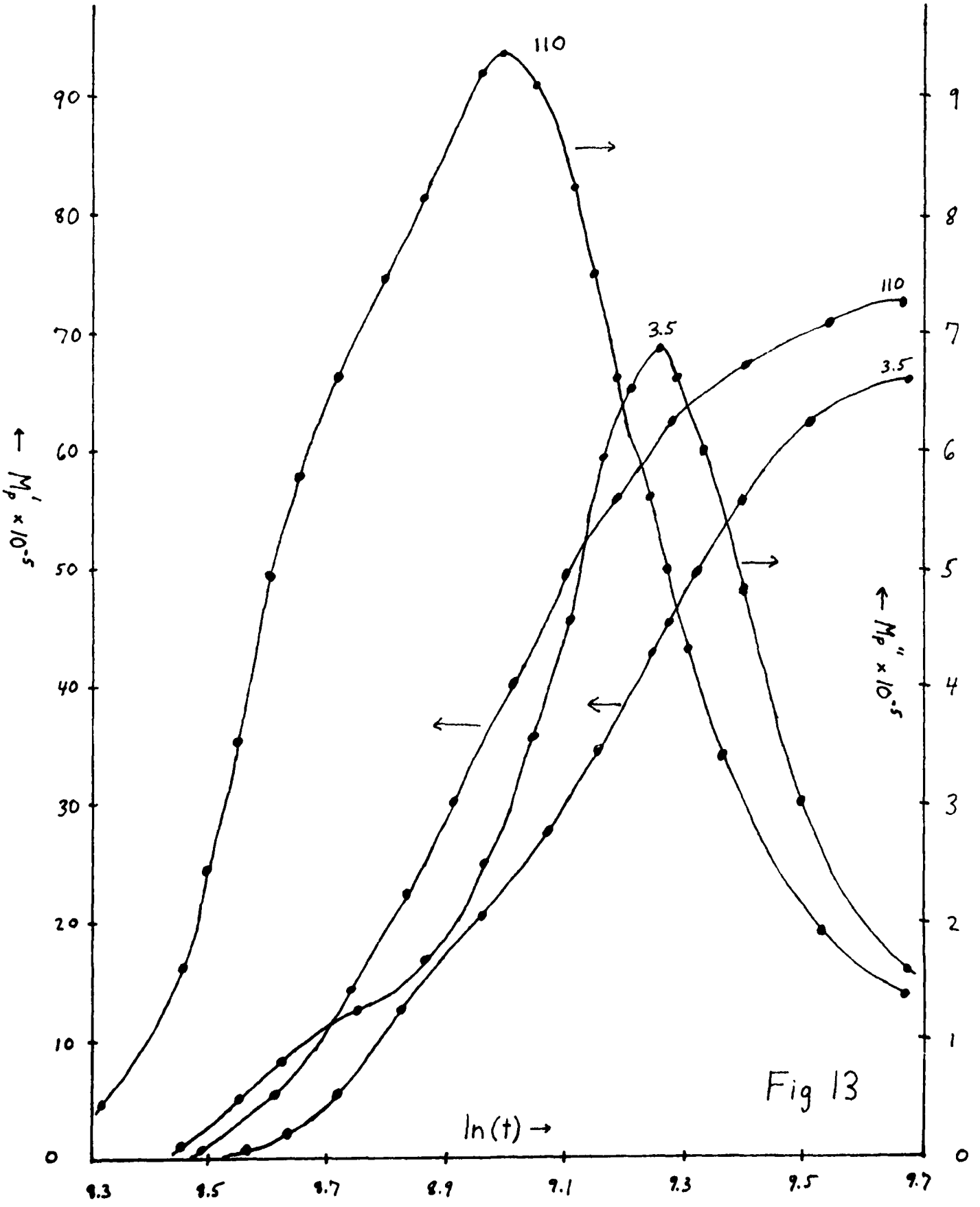
147° C
110
3.5
110
3.5
90
80
70
60
50
40
30
20
10
0
9
8
7
6
5
4
3
2
1
0
↑ $M_p' \times 10^{-5}$
↑ $M_p'' \times 10^{-5}$
ln(t) →
8.3
8.5
8.7
8.9
9.1
9.3
9.5
9.7

Fig 13

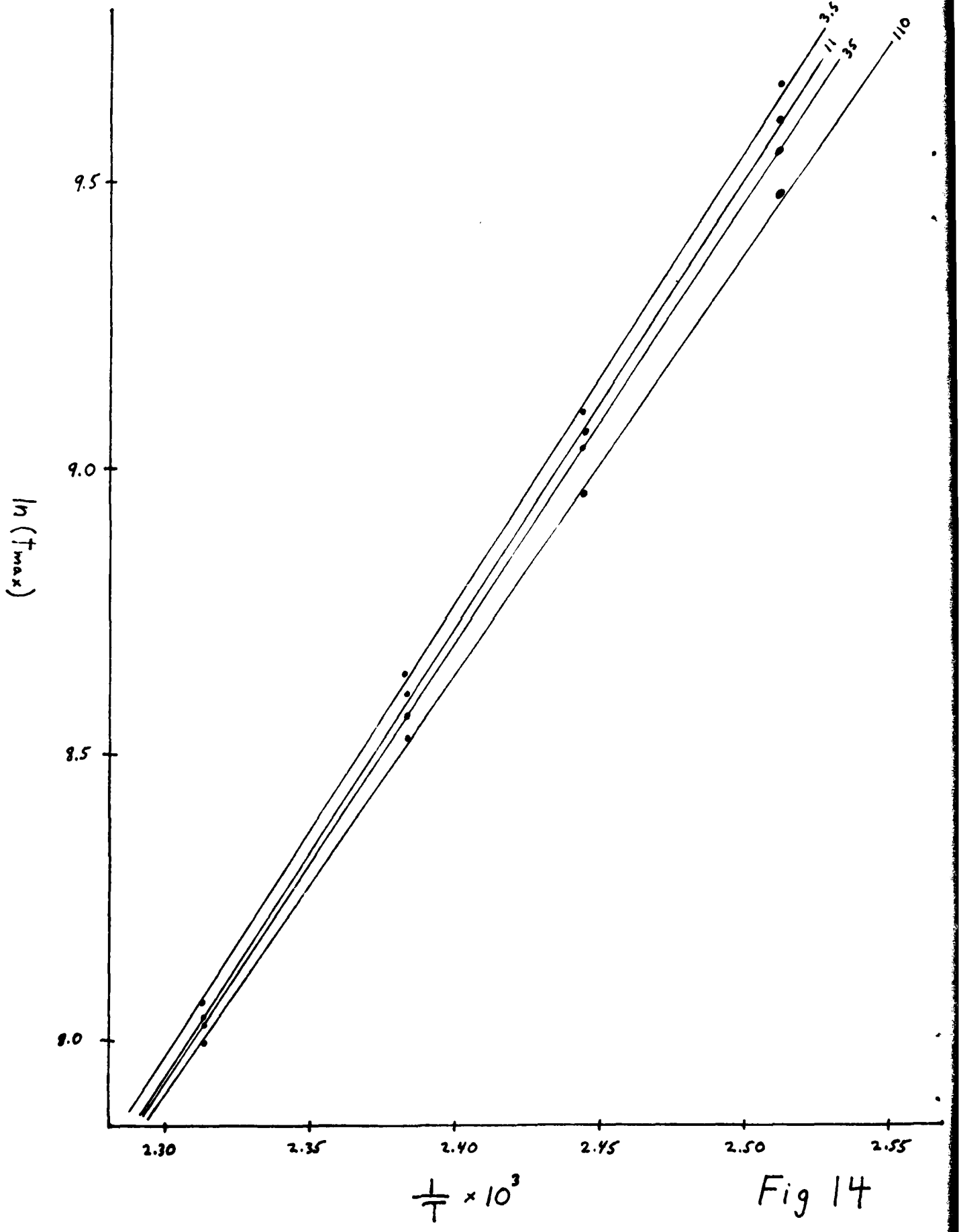

Fig 14

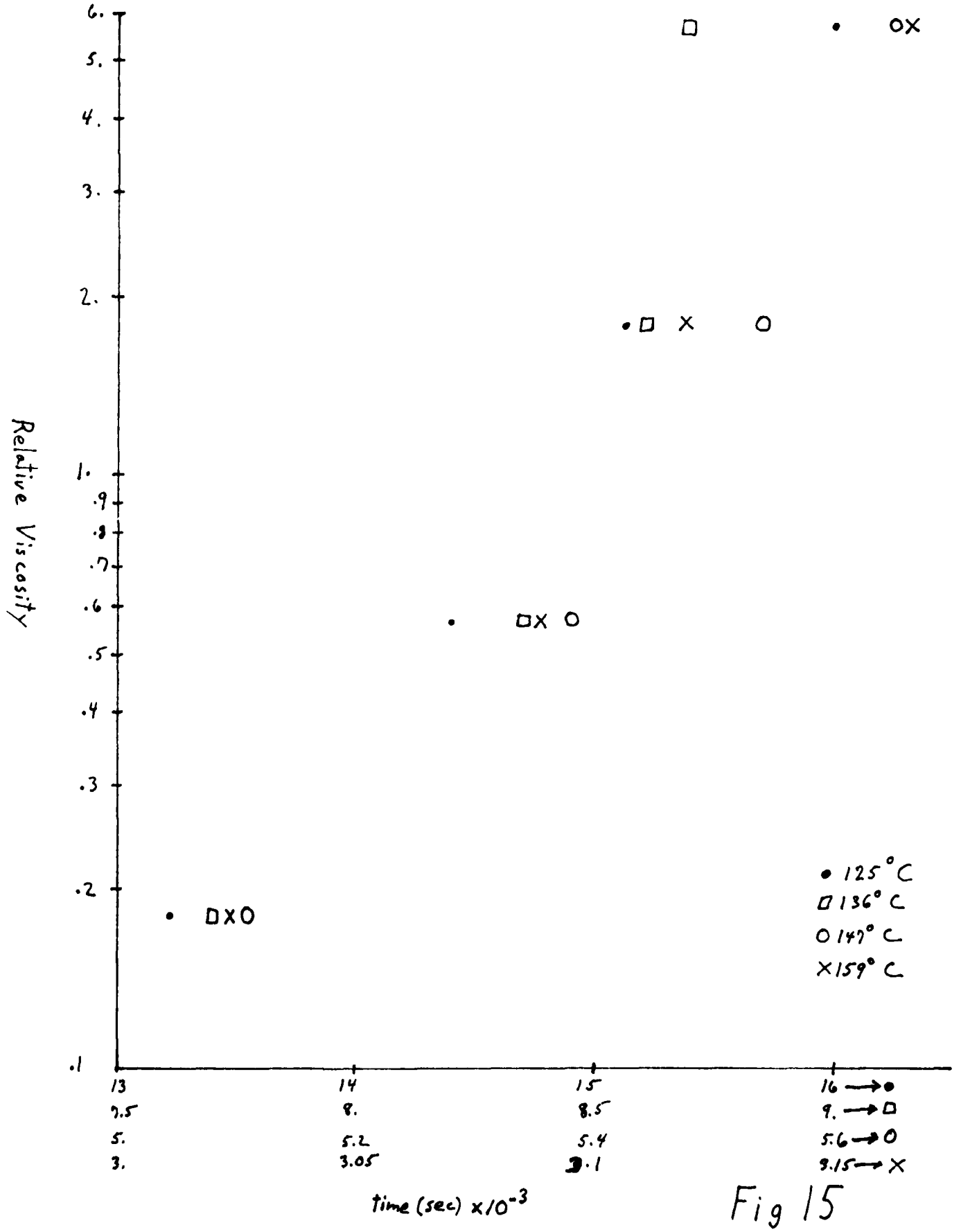
6.
5.
4.
3.
2.
1.
.9
.8
.7
.6
.5
.4
.3
.2
.1
Relative Viscosity
• 125°C
□ 136°C
O 147°C
× 159°C
13
14
15
16 → •
7.5
8.
8.5
9. → □
5.
5.2
5.4
5.6 → O
3.
3.05
3.1
3.15 → ×
time (sec) x10⁻³

Fig 15

DISTRIBUTION LIST

No. of Copies	To
1	Office of the Under Secretary of Defense for Research and Engineering, The Pentagon, Washington, D. C. 20301
12	Commander, Defense Technical Information Center, Cameron Station, Building 5, 5010 Duke Street, Alexandria, Virginia 22314
1	Metals and Ceramics Information Center, Battelle Columbus Laboratories, 505 King Avenue, Columbus, Ohio 43201
	Deputy Chief of Staff, Research, Development, and Acquisition, Headquarters, Department of the Army, Washington, D. C. 20310
1	ATTN: DAMA-ARZ
	Commander, Army Research Office, P. O. Box 12211, Research Triangle Park, North Carolina 27709
1	ATTN: Information Processing Office
	Commander, U. S. Army Materiel Development and Readiness Command, 5001 Eisenhower Avenue, Alexandria, Virginia 22333
1	ATTN: DRCLDC
	Commander, U. S. Army Materiel Systems Analysis Activity, Aberdeen Proving Ground, Maryland 21005
1	ATTN: DRXSY-MP, H. Cohen
	Commander, U. S. Army Electronics Research and Development Command, Fort Monmouth, New Jersey 07703
1	ATTN: DELSD-L
1	DELSD-E
	Commander, U. S. Army Missile Command, Redstone Arsenal, Alabama 35809
1	ATTN: DRSMI-RKP, J. Wright, Bldg. 7574
4	DRSMI-TB, Redstone Scientific Information Center
1	Technical Library
	Commander, U. S. Army Armament Research and Development Command, Dover, New Jersey 07801
2	ATTN: Technical Library
1	DRDAR-SCM, J. D. Corrie
1	DRDAR-QAC-E
1	DRDAR-LCA, Mr. Harry E. Pebly, Jr., PLASTEC, Director
	Commander, U. S. Army Natick Research and Development Command, Natick, Massachusetts 01760
1	ATTN: Technical Library

No. of Copies	To
	Commander, U. S. Army Satellite Communications Agency, Fort Monmouth, New Jersey 07703
1	ATTN: Technical Document Center
	Commander, U. S. Army Tank-Automotive Research and Development Command, Warren, Michigan 48090
1	ATTN: DRDTA-RKA
2	DRDTA-UL, Technical Library
	Commander, White Sands Missile Range, New Mexico 88002
1	ATTN: STEWS-WS-VT
	President, Airborne, Electronics and Special Warfare Board, Fort Bragg, North Carolina 28307
1	ATTN: Library
	Director, U. S. Army Ballistic Research Laboratory, Aberdeen Proving Ground, Maryland 21005
1	ATTN: DRDAR-TSB-S (STINFO)
	Commander, Harry Diamond Laboratories, 2800 Powder Mill Road, Adelphi, Maryland 20783
1	ATTN: Technical Information Office
	Chief, Benet Weapons Laboratory, LCWSL, USA ARRADCOM, Watervliet, New York 12189
1	ATTN: DRDAR-LCB-TL
	Commander, U. S. Army Foreign Science and Technology Center, 220 7th Street, N. E., Charlottesville, Virginia 22901
1	ATTN: Military Tech, Mr. Marley
	Director, Eustis Directorate, U. S. Army Air Mobility Research and Development Laboratory, Fort Eustis, Virginia 23604
1	ATTN: Mr. J. Robinson, DAVDL-E-MOS (AVRADCOM)
	Commander, U. S. Army Agency for Aviation Safety, Fort Rucker, Alabama 36362
1	ATTN: Library, Building 4905
	Commander, USACDC Air Defense Agency, Fort Bliss, Texas 79916
1	ATTN: Technical Library
	Commander, U. S. Army Engineer School, Fort Belvoir, Virginia 22060
1	ATTN: Library
	Naval Research Laboratory, Washington, D. C. 20375
1	ATTN: Dr. J. M. Krafft - Code 5830
2	Dr. G. R. Yoder - Code 6384

No. of Copies	To
	Chief of Naval Research, Arlington, Virginia 22217
1	ATTN: Code 471
	Air Force Materials Laboratory, Wright-Patterson Air Force Base, Ohio 45433
2	ATTN: AFML/MXE/E. Morrissey
1	AFML/LC
1	AFML/LLP/D. M. Forney, Jr.
1	AFML/MBC/Mr. Stanley Schulman
	National Aeronautics and Space Administration, Washington, D. C. 20546
1	ATTN: Mr. B. G. Achhammer
1	Mr. G. C. Deutsch - Code RW
	National Aeronautics and Space Administration, Marshall Space Flight Center, Huntsville, Alabama 35812
1	ATTN: R. J. Schwinghammer, EH01, Dir, M&P Lab
1	Mr. W. A. Wilson, EH41, Bldg. 4612
1	Ship Research Committee, Maritime Transportation Research Board, National Research Council, 2101 Constitution Ave., N. W., Washington, D. C. 20418
	Lockheed-Georgia Company, 86 South Cobb Drive, Marietta, Georgia 30063
1	ATTN: Materials and Processes Engineering Dept. 71-11, Zone 54
	General Dynamics, Convair Aerospace Division, P.O. Box 748, Fort Worth, Texas 76101
1	ATTN: Mfg. Engineering Technical Library
1	Mechanical Properties Data Center, Belfour Stulen Inc., 13917 W. Bay Shore Drive, Traverse City, Michigan 49684
1	Dr. Robert S. Shane, Shane Associates, Inc., 7821 Carrleigh Parkway, Springfield, Virginia 22152
	Director, Army Materials and Mechanics Research Center, Watertown, Massachusetts 02172
2	ATTN: DRXMR-PL
1	DRXMR-PR
1	DRXMR-PD
1	ARXMR-AP
1	Author